# Chloride induced corrision of integral and non-integral surface treated lightweight foamed concrete

By
Admire Ruvimbo Zvinokona

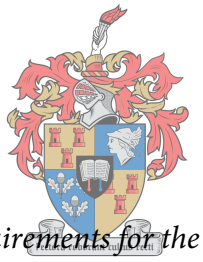

*Thesis presented in fulfilment of the requirements for the degree of Master of Engineering in Civil Engineering in the Faculty of Engineering at Stellenbosch University*




Supervisor: Mr Algurnon van Rooyen

March 2018

## Declaration

By submitting this thesis electronically, I declare that the entirety of the work contained therein is my own, original work, that I am the sole author thereof (save to the extent explicitly otherwise stated), that reproduction and publication thereof by Stellenbosch University will not infringe any third party rights and that I have not previously in its entirety or in part submitted it for obtaining any qualification.

Date: March 2018

## Abstract

Advancement in new technologies and methods of producing foaming agents have resulted in enhanced possibility of a structurally performing lightweight concrete. Lightweight foamed concrete (LWFC) is a cement based composite material that has shown remarkable potential as a replacement to Normal Weight Concrete (NWC) for structural applications. LWFC stands as a low self-weight building material relatively compared to its counterpart, NWC. Other than reduced self-weight, it also possesses desirable properties such as good thermal insulation, excellent fire resistance, and high workability and self-levelling. Technical and engineering unfamiliarity of LWFC has contributed to inhibiting the material's wider use and advancement for structural application. In addition to the above, limited literature on the material's durability properties and performance under exposure to aggressive elements such as carbon dioxide and chlorides contribute as a drawback.

This thesis reports on a durability study on LWFC undertaken at Stellenbosch University (SU). LWFC beam specimens were exposed to cyclic wetting and drying periods using NaCl solution under controlled humidity and temperature conditions. The performance of two types of surface treatment agents in LWFC against preventing accelerated penetration of chloride ions and consequently chloride induced corrosion was the main focus. Chloride penetration was investigated by silver nitrate testing, and reinforcement corrosion was monitored via a non-destructive linear polarisation method using commercially available GECOR 10 corrosion rate measuring equipment.

The results indicated that inclusion of fly ash in reinforced LWFC reduces risk of dry shrinkage cracking, limiting localised corrosion on cracked locations. The surface applied silane-based water repellent treatment agent was effective in preventing moisture penetration, leading to the low reinforcement corrosion rates and chloride ion penetration depths.

## Acknowledgements

I would like to expresses my gratitude to the following people and organisations for their valuable contributions to this research study:

- My supervisor, Mr. Algurnon Van Rooyen, for his guidance, encouragement and support throughout this study.
- Sika South Africa – Sika group, for their materials sponsorship, in particular the waterproofing admixture for mortar that was used throughout this study.
- The Concrete Institute for their funding to my entire masters study
- Miss Monalisa C. Mataure, my wife to be, for her support, encouragement and patience with me during my study period.
- Mr. Tinotendaishe D. Muzofa, Mr. Monwabisi C. Langa, and Mr. Tasimba Chirindo, for their true friendship, encouragement, honest criticism, scrutiny and support while I worked on this project.

Lastly I would like to thank all the staff members at the Structural Engineering and Civil Engineering Informatics division, with special mention to, Mr. J van der Merwe, Mr. C Ramat and Mr P Cupido for their meticulous help during the construction and testing phase.

# Dedications

*I dedicate this thesis to my wife to be, Monalisa C. Mataure and our unborn child.*

# Contents

# List of Figures

# List of Tables

# Nomenclature

## Abbreviations

| | |
|---|---|
| ASR | Alkali-Silica Reaction |
| C-S-H | Calcium Silicate Hydrate |
| IT | Integral treatment |
| LPR | Linear polarisation resistance |
| LWFC | Lightweight foamed concrete |
| NaCl | Sodium chloride solution |
| NWC | Normal weight concrete |
| REF | Reference |
| R/LWFC | Reinforced Lightweight foamed concrete |
| STAs | Surface treatment agents |
| ST | Surface treatment |

# List of Symbols

| | |
|---|---|
| $Rp$ | Polarisation resistance |
| $\Delta E$ | Potential difference |
| $\Delta I$ | Current difference |
| $I_{corr}$ | Corrosion current density |
| $I$ | Electrochemical reaction current |
| $I_o$ | Exchange current |
| $E$ | Electrode potential |
| $E_o$ | Equilibrium potential |
| $\beta$ | Tafel constant |
| $\beta_c$ | Cathodic Tafel constant |
| $\beta_a$ | Anodic Tafel constant |
| $Q$ | Electrical charge |
| $n$ | Electron charge |
| $F$ | Faraday constant |
| $M$ | Number of moles |
| $m$ | Mass |
| $t$ | Time |
| $M_r$ | Molecular weight of an element |
| $f_{cu}$ | Compressive strength |
| $F_s$ | Maximum compressive force |
| $A$ | Specimen cross-sectional area |
| $p$ | Porosity |
| $y_d$ | Dry density [kg/m$^3$] |
| $f_p$ | Cube compressive strength of paste [MPa] |
| $f_{fc}$ | Compressive strength of foamed concrete [MPa] |
| $\alpha_b$ | Binder ratio |
| $\rho_m$ | Target casting density [kg/m$^3$] |

| | |
|---|---|
| x | Cement content [kg/m$^3$] |
| $\frac{w}{c}$ | Water to cement ratio |
| $\frac{a}{c}$ | Ash to cement ratio |
| $\frac{s}{c}$ | Sand to cement ratio |
| $\frac{w}{s}$ | Water to sand ratio |
| $RD_f$ | Relative density of foam [kg/m$^3$] |
| $RD_c$ | Relative density of cement [kg/m$^3$] |
| $RD_a$ | Relative density of ash [kg/m$^3$] |
| $RD_s$ | Relative density of sand [kg/m$^3$] |
| $V_f$ | Volume of foam[l] |

# 1 Chapter One

## 1.1 General Discussion

Lightweight foamed concrete (LWFC) offers an appreciably lower density concrete as compared to the usual concrete produced from normal weight raw materials/aggregates. This research study focuses on the durability properties of lightweight foamed concrete, which is produced by a method of introducing air-voids into a cement paste consisting of cement, water, fibres and fly ash. The creation of air-voids in a cement paste is achieved by adding foam into the paste. The foam is produced from a protein/synthetic foaming agent which is diluted with water and aerated to form the foam (Panesar, 2013).

The use and development of lightweight foamed concrete dates back to the early 1900's. Since then foamed concrete has been mainly implemented in non-structural applications owing to its technical and engineering unfamiliarity and a perceived difficulty of attaining high compressive strength (Jones & McCarthy, 2005). Durability of LWFC is also another factor that has stalled its further advancement in wider structural application. The main aggressive elements that threaten the durability of steel in reinforced concrete are chloride ions, carbon dioxide and sulphur oxides. Water and oxygen are also considered as critical elements that work hand in hand with the aforementioned aggressive elements in causing damage to reinforcement in concrete structures. Water is said to provide the medium for transport of aggressive elements (chloride ions) in solution and also aids on establishing electrolytic continuity inside the concrete, a condition that favours corrosion to continue taking place once initiated.

Due to the wide spread use of concrete in structures, including in environments that are aggressive, there is an increasing need to provide alternative measures to protect the concrete from aggressive elements.

These environments include marine areas and their proximities, and chloride-induced permeable environments (i.e. where de-icing salts are used). Generally when concrete structures' surfaces come into contact with water containing aggressive elements, the solution is taken up quickly by capillary suction. The aggressive elements are further transported into the concrete by a process called diffusion which is relatively slower than

capillary suction. Once the aggressive elements' concentration e.g. chloride reaches a critical level on the area surrounding the reinforcement, deterioration via corrosion of the steel is initiated. Thereafter corrosion will progress at a faster rate provided the conditions remain favourable. The reinforcement suffers significant loss of strength and cross-sectional area which in turn affect the structural capacity of a reinforced structure or member leading to catastrophic failure (Neville, 1995).

Previous research indicates that the use of surface treatment agents (STAs) notably reduces aggressive element penetration in concrete structures therefore limiting associated damages like corrosion of reinforcing steel (Medeiros & Helene, 2009). The main role for surface treatment agents in concrete is to alter the surface layer properties so that the conditions for aggressive element transport and fixation of moistures are not favourable. In a way this reduces the damage to the structures by penetration of aggressive elements to the reinforcement level. The efficiency of these surface treatment agents is also affected by proper use, handling and application of guidelines when dealing with the products. Proper consideration must be taken during application, application methods used and special treatment before or after application.

Nevertheless there is limited literature and research data available on the use and efficacy of surface treatment agents in foamed concrete. Hence this research will focus on the aspect of investigating the use of surface treatment agents against chloride penetration in foamed concrete.

## 1.2 Problem Statement

Lightweight foamed concrete has proved to be a promising material towards replacing normal weight concrete in semi structural applications. Comparable strength capacities to those of normal weight concrete can now be achieved as a result of the advances in the design procedure and foam production methods. Since there has been a breakthrough of the material's strength capabilities, the drawback towards replacing normal weight concrete in reinforced structural application of the material has been on its durability capabilities. The generally unavoidable interaction of the concrete surface with the external surroundings containing aggressive elements in different forms raises serious durability concerns of the materials if it is to be successfully implemented for structural purposes.

LWFCs' microstructure is very porous as a result of entrained air-voids (Kearsley & Wainwright, 2001a). This property creates the perception that the material is susceptible to increased rate of penetration by moisture, ions and gases that compromise its durability. In order to advance the application of LWFC concrete particularly in reinforced elements or members, more information is needed to understand how the material performs with regards to durability and also explore alternative measures to enhance durability under exposure to aggressive elements.

For this reason evaluation of the efficacy of alternative measures, which enhance durability of reinforced concrete, is of utter most importance. This study builds on the foundation of investigating the performance of surface treatment agents against chloride induced corrosion. This is done in order try and contribute knowledge and data that can be part of advancing the use of LWFC for structural purposes.

## 1.3 Research Scope

The research was initiated to generate and add information with regards to the efficiency of selected surface treatment agents, chloride ingress in LWFC, and corrosion of reinforcement. Some supporting study such as long term compressive strength of LWFC with fly ash content (fly ash: cement ratio of 2:1) was also conducted.

A commercially available GECOR 10 corrosion rate measuring equipment was used for determining the corrosion rate of the reinforcement in LWFC and chloride penetration depths were determined using the silver nitrate discoloration test. This research will mainly focus on the durability performance and enhancement of LWFC by use of two locally available surface treatment agents in South Africa.

## 1.4 Research Objectives

The objectives of this study can be summarised as follows:

- To contribute towards further acceptance of foamed concrete as an alternative to normal weight concrete in semi-structural applications,
- To assess and evaluate the durability properties of foamed concrete, in particular resistance against chloride penetration,
- To evaluate the efficacy of surface treatment in foamed concrete,

- And finally, to determine the effect of cracks and fly ash inclusion in foamed concrete with regards to reinforcement corrosion

## 1.5 Limitations of the Research

This study was limited to investigating the performance of STAs on reducing the corrosion rate in reinforced LWFC. The STAs used in the research study are locally available commercial products from Sika®. Two types of surface treatment agents were investigated:

i) A waterproofing admixture for mortar called Sikalite, which is a powder-like product and is applied as a percentage of cement content with the dry aggregates.
ii) A surface applied silane-based water repellent impregnation cream called Thixo 706. It is applied on to the surface of the beams after the curing period.

The wet target density of the LWFC used for experimental specimen production was 1600 kg/m3.

## 1.6 Summary

The development of LWFC properties via improved methods of foam production brings new possibilities of a wider application of the product as a load bearing structural building material. Though previous researchers have proved that high strengths comparable to that of NWC can be attained with LWFC, questions still remain about the durability properties and capabilities of LWFC. Hence the need to investigate its properties with regards to attack by common aggressive elements encountered when concrete is exposed to the environment. It is also worth mentioning that there exist structural buildings that are in use where LWFC was the main building material. However the question still remains, what is the durability confidence of the material given its high level of porosity and, if need be, what can be done to improve its durability performance.

## 1.7 Thesis Layout

The first chapter gave a brief background of the rationale behind using surface treatment agents to enhance the durability of LWFC. The scope and limitations of the research

investigation were established and the specific problem statement was defined. Chapter 2 presents the literature review of surface treatment agents' application and functional mechanisms in concrete. It concludes by highlighting the factors affecting performance of surface treatments in concrete.

In Chapter 3, the theory behind the corrosion rate measuring technique used in this study is discussed. The chapter starts off with a brief discussion of the corrosion rate background, followed by an in depth review of the method used in this study. The second half of the chapter focuses on the results interpretation of the corrosion rate measuring technique used and how they can be interpreted in engineering context. It derives the relationship between the electrochemical data for corrosion measurement and the engineering terms or concepts.

Chapter 4 gives the experimental design procedure of the study. The materials used to prepare the LWFC are specified and the preparation procedure is discussed. The experimental tests and method of testing done in this study are also discussed including the tested parameters.

Chapter 5 includes the final discussion on all the results obtained from the experimental tests conducted. And Chapter 6 zones in on the conclusions made and gives a list of recommendations for future study.

# 2 Chapter Two

# Literature Review

## 2.1 Introduction

This chapter provides in detail the types of surface treatments agents (STAs) available for application in concrete. The STAs are discussed in terms of their functionality, protection mechanism and application methods. A focus on the practical implementation of the treatment agents is also included. The factors affecting the performance of the treatment agents are also discussed, with reference to product manufactures' recommendations and previous academic research conducted. A brief background on LWFC is presented first.

## 2.2 Lightweight Foamed Concrete (LWFC)

Lightweight foamed concrete (LWFC) is a homogenous material composed of fine aggregates or fillers (e.g. sand/lime), cement and cement extenders and entrapped air (Bach, Bormann, Kucharski, & Wilk, 2004). It can also incorporate light weight aggregates such as furnace clinker, blast furnace slag, expanded clay, shale and slate. The light weight aspect in LWFC is as a result of entrapment of between 10% and 70% air voids (Panesar, 2013).

The selection criteria for various applications of LWFC are based mainly on air-dry-density which heavily influences its strength. The air-dry-density ranges between 300 and 1800 kg/m$^3$ as opposed to normal weight concrete with density in the region of 2350 kg/m$^3$ (Alexander & Beushausen, 2009). LWFC is reported to possess superior properties such as; a higher strength to density ratio, self-levelling capabilities, better thermal and acoustic properties due to its textural surface and micro-structure, and a rigid well bound body after hydrating.

However, its wider use in structural applications has been hindered by its technical and engineering unfamiliarity. Some characteristics such as relatively low tensile strength and high drying shrinkage strains have also contributed to the drawback (Jones & McCarthy, 2005).

Over the past years, improvements in the production methods of foaming agents resulting in enhanced properties gave rise to interest in the load bearing structural application of LWFC.

The mechanical properties suitable for structural application have been achieved for densities ranging between 1200 to 1600 kg/m$^3$. However, due to its porous microstructure, concerns have been raised regarding penetrability by aggressive elements (e.g. chloride ions) and gasses which compromise the durability performance of the material.

If LWFC is to be utilized on a large scale the durability performance first needs to be understood. Limited research exists on LWFC durability performance, and this study will look at adding knowledge on durability enhancement against chloride induced corrosion by use of surface treatment agents.

## 2.3 Surface Treatment Agents in Concrete

### 2.3.1 Introduction

Various reasons exist for the application of STAs on concrete structures. The reasons are motivated by either poor material performance (i.e. permeability and abrasion) or harsh exposure conditions. Applying surface treatments on concrete can be a preventative measure, on which the goal will be to prevent deterioration of concrete against acid attack, weathering, or reinforcement corrosion. The point behind using the surface treatments is to alter the properties of concrete, consequently changing the circumstances of transportation and fixation of moisture and deleterious elements. Surface treatments can also act as limiting agents to the rate of deterioration of reinforced concrete via corrosion or alkaline silicate reactions.

Other reasons for use or application of surface treatments not related to durability performance include; appearance (colour & surface texture), aesthetic, defect concealment (efflorescence & stains). If placement, compaction and curing is done properly, concrete on its own is regarded as a durable material, however it should be noted that the application of surface treatment can become a necessity in order to achieve a requested service life under certain exposure conditions which may be highly aggressive.

With regards to durability performance, surface treatments have high potential to increase the deterioration/corrosion initiation period by limiting the transportation of aggressive elements or compounds within the concrete. Such elements include chloride ions, sulphates, and carbon dioxide. In concrete structures where degradation has already started, surface

treatments can be used to reduce the rate of deterioration by limiting penetration of essential elements required for the deterioration process to continue (e.g. corrosion), consequently increasing the service life of the structure.

Each structure, based on its exposure condition and purpose, requires a specific type of surface treatment. The properties of surface treatment agents differ based on the type(s) of materials and compounds they are manufactured from. It is important to ascertain whether any product considered for application meets the anticipated properties and will not conflict with the properties of the material on which they are applied. To achieve intended the performance of surface treatments it is also important that they are applied onto concrete structures in the correct manner and that the surface preparation of the concrete is correctly done.

Surface treatment systems incorporating several products can be considered in very aggressive environments (Basheer, Basheer, Cleland, & Long, 1997).

For example, a system of coatings and hydrophobic impregnation can be applied to a concrete structure, in which the hydrophobic impregnation will ensure low moisture penetration on defective surfaces of the concrete for example cracked concrete surfaces, where the coating protective mechanism would have been affected by the crack.

## 2.4 Surface Treatment Agents Classification

Surface treatment agents can be classified according to their main generic component, functional or protection mechanism, curing requirements, or properties such as degree of penetration and thickness of the surface film. Based on EN 1504-2 (2004) and the protection mechanism, surface treatment agents can be classified into three main groups: Coatings (e.g. bitumen), Pore liners (Hydrophobic impregnation), and blocker (Impregnation) (Medeiros et al., 2012) see Figure 1.

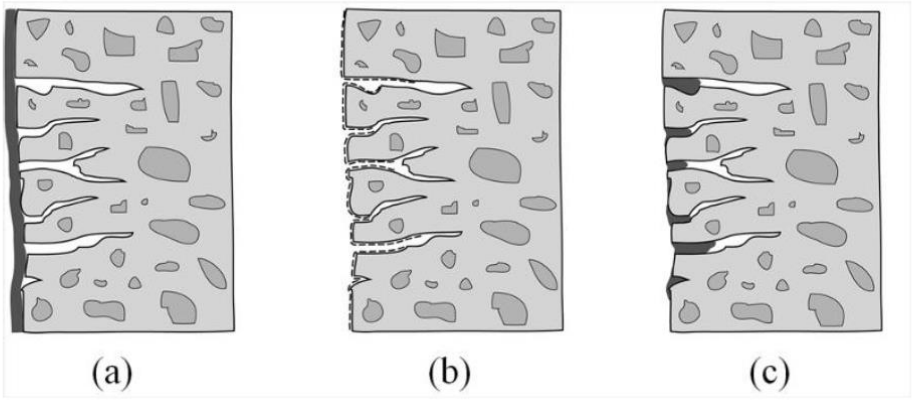


Figure 1: Surface treatment protections (a) coating and sealers (b) pore liner (c) pore blocker (Medeiros et al., 2012)

### 2.4.1 Pore liner (Hydrophobic impregnation)

Technically called hydrophobic agents. They penetrate into the concrete surface pores and react with the hydrated cement particles forming a water-repellent surface lining protection without a pore filling effect (Franzoni, Pigino, & Pistolesi, 2013).

Hydrophobic agents are organic polymers made up of different organic groups (silicon resins) of varying chain lengths, they are mainly composed of either silane or siloxane organic compounds.

Irrespective of the composition of a specific product, the water repellent by-products that result from the chemical reaction of the concrete surface and the agents are called silicone (Giessler, Standke, & Büchler, 2005; Medeiros & Helene, 2009; Sikagard ® -706 Thixo, 2012; Tittarelli & Moriconi, 2010). Figure 2 depicts a typical silicone by-product formed on a concrete surface.

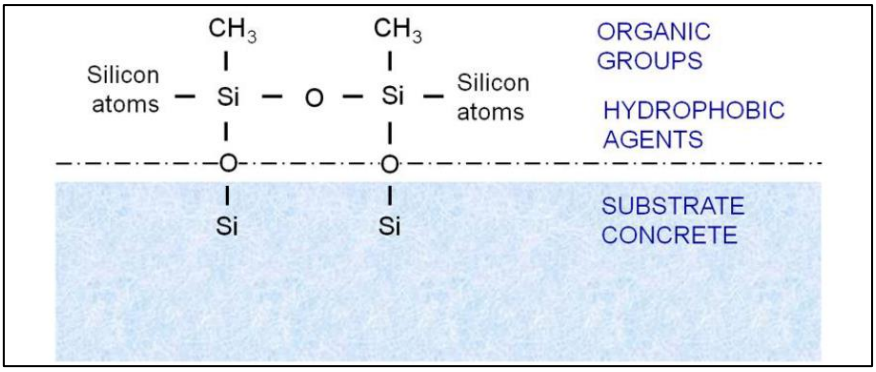


Figure 2: Schematic representation of a chemically bonded hydrophobic agent to a concrete substrate (Medeiros et al., 2012)

### *2.4.1.1 Hydrophobic impregnation protection mechanism*

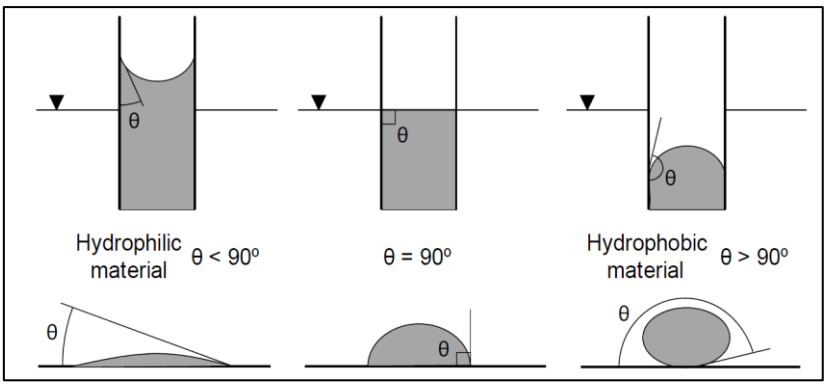


Figure 3: Difference between a hydrophilic and a hydrophobic material in terms of capillary forces and exposure to water (Selander, 2010)

The mechanism which describes the water repelling action of hydrophobic agents is referred to as the lotus effect and it is illustrated in Figure 3. Concrete on its own is a hydrophilic material hence when it comes in contact with water, its contact angle is often considered to be zero or less than 90°. This means that the pore structure of concrete generates capillary forces that draw water into their system when in contact.

A change from hydrophilic to hydrophobic properties occurs on the concrete surface when it is treated with a water repellent agent, Figure 3. According to Giessler et al. (2005), in contrast to the action of coatings, the surface pores and breathability of the concrete remain unaffected, leaving the movement of gases (e.g. water vapour) into and out of the concrete

entirely unaffected. This mechanism is effective in stopping the penetration of liquids transporting deleterious elements into concrete for example chloride ions.

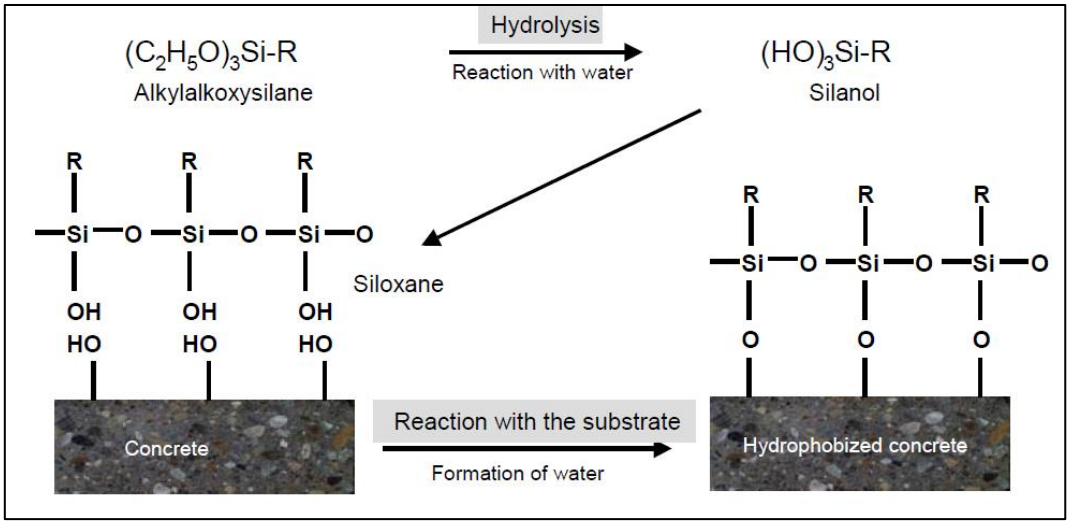


Figure 4: Schematic representation of the change from hydrophilic to hydrophobic of the surface of concrete when it comes in contact with a water repellent agent (Giessler et al., 2005)

Figure 4 depicts the chemical reaction process of a hydrophobic agent and a concrete surface step by step. The untreated surface (concrete) is hydrophilic because of the hydroxyl ions on the surface.

The hydrophilic surface is altered when the siloxane polymer from a water repellent agent is applied, resulting in a hydrophobic state (hydrophobized concrete).

### 2.4.2 Pore blocker (Impregnation)

Pore blocker products react with soluble constituents in the concrete pore structure to form insoluble by-products that block the concrete pore system. They resist penetration of concrete by liquids under a pressure gradient. Pore blockers are mainly composed of inorganic silicates for example sodium silicates, potassium silicates, and fluorosilicates (Jia, Shi, Pan, Zhang, & Wu, 2016), chemically inorganic-organic compounds namely ethyl silicate also exists. Equation (2.1) depicts the chemical reaction of a sodium silicate based product inside the concrete pore structure.

$$Na_2SiO_2 + yH_2O + xCa(OH)_2 \rightarrow xCaO.SiO_2.yH_2O + 2NaOH \qquad (2.1)$$

A less porous concrete pore structure results due to the precipitation of $SiO_2$. With reference to Equation 2.1, Medeiros et al. (2012) mention that the presence of portlandite ($Ca(OH)_2$) is crucial for the reaction to take place. The authors further highlight that for the reaction to occur, sufficient presence of portlandite is of utmost importance. This results in a carbonation resistant concrete due to the reduced portlandite content or concentation which is a crucial reactant in the carbonation process (Aguiar & Junior, 2013).

#### *2.4.2.1 Impregnation protection mechanism*

The silicates found in the pore blocker products chemically react with portlandite producing a precipitate of a silica gel and sodium hydroxide inside the material's porous microstructure. In Equation 2.1 a calcium silicate hydrate (C-S-H) gel is produced. This results in improvement of concrete hardness and decrease in permeability of the concrete layer, which comes as a result of the gel that fills the pores of the concrete (Franzoni et al., 2013; Pigino, Leemann, Franzoni, & Lura, 2012; Sandrolini et al., 2012).

Figure 5 presents the reaction scheme of an inorganic-organic ethyl silicate to form a pore blocking silica gel inside a concrete pore structure.

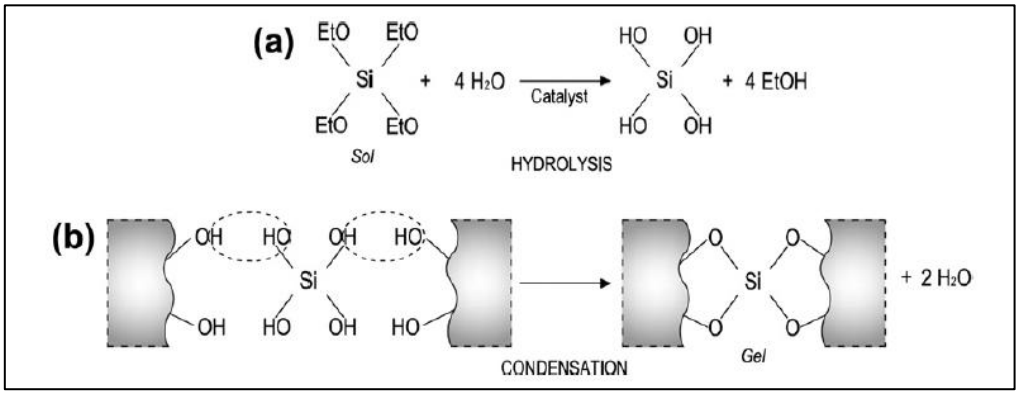


Figure 5: Ethyl silicate reaction scheme: (a) hydrolysis reaction (b) condensation reaction on the substrate surface to form silica gel (Sandrolini et al., 2012)

### 2.4.3 Coatings

This type of surface treatment agent forms a continuous film on the concrete surface, shielding it completely from the external environment exposure. In coatings, some product manufacturers may recommend that multiple layers be applied to improve the protection performance of the material. On the other hand, performance of any surface protection

system is dependent also on exposure conditions, which heavily influence the selection choice of a type of coating to use. Coatings are mainly composed of epoxies, polyurethane, vinyl, acryl, chlorinated rubber, styrene butadiene, cement and bitumen.

## 2.5 Protective Functions

The choice of a surface treatment mechanism to be applied on a structure should be based on the assessment of the actual or potential causes of deterioration. Moisture is a critical factor in chloride induced corrosion processes as it is the medium of transportation of deleterious elements in concrete. In the absence of moisture, the corrosion process will not proceed or will significantly slow down.

One possible way of preventing deterioration of reinforced concrete structures is to prevent transportation of moisture and gases containing deleterious elements into the concrete. Hence the ability of a surface treatment to control moisture content inside the concrete is of paramount importance and value.

### 2.5.1 Chloride corrosion

Chloride induced corrosion of embedded reinforcement in concrete is one of the main deterioration problems experienced in reinforced structures. The mechanism behind the deterioration process is complex, although it is understood that chloride ions destroy the protective film surrounding the reinforcement formed by the alkaline environment in concrete. For chloride ions to reach the level of reinforcement, they travel through the concrete matrix in solution via the transport mechanisms. The ability of surface treatments to limit the moisture transport into concrete prevents the movement of chloride ions to the level of reinforcement.

Moisture content inside the concrete is an essential parameter in the corrosion process, it acts as an electrolyte providing a transport medium for hydroxyl ions from the cathodic to the anodic region where the corrosion products are formed. Hence the capability of a surface treatment to prevent further corrosion is dependent on its ability to limiting further ingress of moisture into the concrete. By limiting moisture ingress, the amount of electrolytes inside the concrete is reduced and chloride transport is inhibited, which results in an increase of the electrical resistivity of the concrete and reduced corrosion rate.

### 2.5.2 Carbonation induced corrosion

By limiting carbon dioxide penetration into concrete, surface treatment agents can retard the carbonation process, thus maintaining the passive environment around the reinforcement. The corrosion process caused by carbon dioxide is related to the reduction of the alkaline environment around the reinforcement.

When carbon dioxide penetrates the concrete, it reacts with the hydration products (carbonation reaction) which results in the reduction of the pH levels inside the concrete. Reduction in the pH level in the surrounding environments of the reinforcement results in the destruction of the passivity layer around steel making it prone to corrosion.

Since surface treatments can reduce the moisture content within the concrete, it is also important to note that carbon dioxide diffusion into the concrete is high at low moisture content which equates to a high carbonation rate. The maximum carbonation rate occurs at a relative humidity of 70% (Utgenannt, 2004), Figure 6.

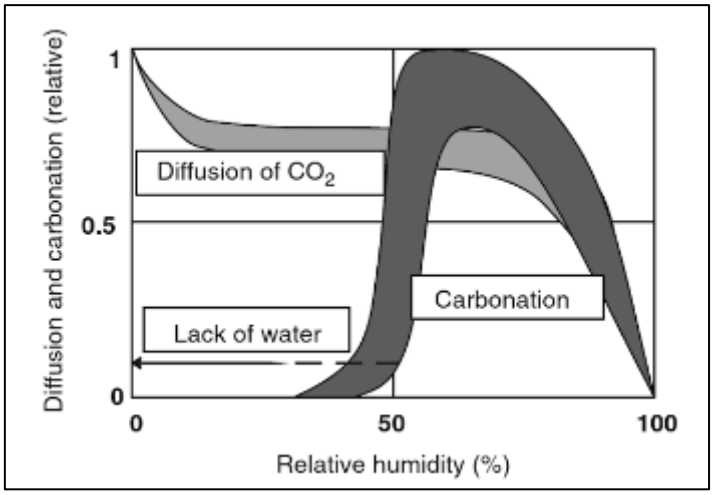


Figure 6: Relative diffusion coefficient of carbon dioxide and relative rate of carbonation as a function of relative humidity (Böhni, 2005)

Most effective surface treatments against carbon dioxide related corrosion are the ones that absorb the carbon dioxide, forming a sacrificial mechanism of protection for example cementitious mortars or coatings. Figure 6 is a simplified sketch for the relationship between carbon dioxide diffusion coefficient and relative humidity in the concrete.

### 2.5.3 Alkali-silica reactions

Alkali-silica reactions (ASR) is an expansive product resulting from the reaction between alkalis (from cement hydration) and silica containing aggregates. This reaction is affected by the moisture content inside the concrete. The moisture has a capacity of transporting the alkalis to the reactive aggregates thereby initiating the reaction. As mentioned earlier, the ASR gel like product is expansive, it induces pressure within the concrete enough to cause cracking (Otieno, 2010).

In saturated concrete with very high moisture content, there is a possibility of this ASR gel product to penetrate the pore system of the concrete with low viscosity and resulting in low expansive pressure. According to Albert (2017), application of a saline surface treatment on concrete slows the development of ASR deterioration as a result of a reduced moisture state inside the concrete. Limit the moisture content in concrete reduces the transport effect of alkalis to the reactive aggregate, hence minimising the possibility of crack formation in concrete.

### 2.5.4 Frost damage

Frost damage in concrete can be divided into two categories; internal and external. Internal frost damage occurs when the water/moisture inside the concrete pore structure freezes thereby resulting in cracking as a result of stresses due to increase in the volume (9% expansion when liquid water turns to ice). External damage however occurs when the concrete surface freezes resulting in deferential stresses between the surface and the internal matrix of the concrete (Fridh, 2005). This type of damage (external) is well known as ‘salt frost scaling’, and it is common in very cold environments where salt is used to deice surfaces (pavements).

Surface treatments can be used to prevent the penetration of moisture into the concrete, hence reducing the probability of internal frost damage.

A three-year field evaluation of saline applied concrete pavements conducted by Albert (2017) indicated that saline treatment on concrete slowed down the deterioration, as a result of freezing and thawing action, by reducing the moisture state of concrete.

The ability of surface treatments to prevent any further moisture penetration into the concrete is of great value in cases were frost damage is more likely to happen. In addition, some surface treatments allow water vapour permeability so that entrapped moisture can leave the concrete to avoid internal frost damage e.g. hydrophobic surface treatments (Selander, 2010).

### 2.5.5 Abrasion damage

Weak surfaces are common in concrete structures. They arise due to poor casting or weathering. The use of surface coatings and pore blockers can increase the abrasion resistance of worn surfaces. The surface treatments that may be applied to or prescribed should possess abrasion and impact resistance properties.

## 2.6 General Aspects of Surface Treatments Based on Protective Function

From the research presented in Sections 2.3 to 2.4.2.1, it can be concluded that the effective protective mechanism lies mainly in the capability of a product to limit the penetration of moisture into the concrete. However, diffusion of water vapour through the surface treatments is an important factor as this will help with maintaining a favourable moisture content within the concrete by avoiding entrapment.

Cracking in concrete is also another aspect that will affect the performance of surface treatments. Hence crack bridging possibilities in concrete through use of fibres is an important aspect to consider in cases where aggressive elements penetrate the concrete in solution e.g. chlorides. Other aspects of surface protection systems that need to be considered based on the exposure environment and prescription are; fire resistance, strength, thermal expansion, and shrinkage.

The protection efficiency of surface treatments against chloride and carbon dioxide penetration may deteriorate with time. Therefore product durability conditions and performance should always be prescribed as well as monitored with time.

## 2.7 Durability and Serviceability of Surface Treatments

The durability and serviceability of surface treatments are affected by exposure conditions, type of structure, application method, choice of treatment and its properties. Hence these factors need to be taken into account when selecting a specific product for application.

For most surface treatment products, if not all, there exists an application method to be followed. These methods are crafted by manufacturers based on large amounts of laboratory tests and trials. However, site conditions vary significantly with laboratory conditions but acceptable levels of protection can be attained if procedures are followed. Exposure conditions and UV light can affect the durability of surface treatments for a long period of time, depending on their properties and interaction with the concrete.

The durability of hydrophobic treatments is dependent on two main factors, which are: surface exposure and penetration depth. According to Selander (2010), the resistance to surface exposure elements is sensitive to the environment and loading factors and disappears within a year, yet the penetration depth factor can last for a long period given that sufficient depth is reached. Hydrophobic impregnations have a capability of penetrating the pore structure of concrete, meaning enhanced exposure resistance to environmental factors such as UV light can be attained, resulting in prolonged durability.

Properties, such as water vapour permeability by hydrophobic impregnation enhance the durability of the surface treatments against delamination.

Surface treatment agent delamination may arise as result from moisture accumulation in concrete underneath the surface treatment. Hydrophobic surface treatments offer excellent serviceability in concrete structures as they do not alter the appearance of the surfaces to which they are applied.

Coatings have been used for long periods of time and their application methods heavily impact durability and serviceability. Blisters and abrasion are common durability problems associated with coatings. Though all surface treatments are sensitive to quality application and preparation of the concrete surface, coatings are the most affected in this regard. Poorly prepared surfaces and substandard workmanship significantly affect coatings. The commonly

affected property of coating treatments, and arguably the most important one, is its adhesion to the concrete surface.

Coatings pose a risk of moisture accumulation underneath the concrete surface, which can lead to loss of adhesion of the coating to the surface. Coatings tend to alter the aesthetic appearance of the surface to which they are applied, a factor that may compromise the attractiveness of a structure. However, they offer a broad variety of colours to choose from, a factor that offers possibilities to capitalise on an alternative aesthetic appearance of a structure. Coating degradation may also result from temperature cycling and shrinkage, which can cause internal stresses in the surface treatment. A repair involving coatings will always result in a change in the aesthetic appearance of the repaired structure.

In conclusion, the durability and serviceability of surface treatments is a combination of various factors that need to be considered together for effective performance of any product. It is important that surface treatments can resist deterioration as a result of outdoor exposure (UV-radiation, pollutants and acid rain) as these conditions may lead to the loss of the functional properties of the treatment agent (Franzoni et al., 2013).

## 2.8 Substrate Preparation and Application of Surface Treatments

Clean substrate (concrete surface) free from contamination by grease, oil, loose materials, and curing products offer satisfactory adhesion and penetration of surface treatments (Raupach & RÖßLER, 2005). Insufficient adhesion is common on substrates with oil remains, a primer may be required in some cases (weak surfaces) for improved adhesion. A few examples of cleaning methods for concrete surfaces include:

> Washing with water, steam cleaning, pressurised air cleaning, pressurised water cleaning, sandblasting, flame cleaning, mechanical cleaning, and chemical cleaning.

Information on acceptable cleaning methods relative to a respective surface treatment is mainly prescribed by the product manufacturer and usually contained in the product data sheet (See appendix E on page 74) (Sikagard ® -706 Thixo, 2012).

## 2.9 Application Factors Affecting Performance of Surface Treatments

### 2.9.1 Hydrophobic treatments

#### *2.9.1.1 Penetration depth*

Performance of surface applied treatment agents is linked to the penetration depth of the product into the concrete substrate. Depending on the type of a product, most product data sheets prescribe a minimum penetration depth or thickness for effective performance of the treatment. The penetration depth can be a minimum of 2mm (Johansson et al. 2005), or 4mm (Zhan & Wittmann, 2005) to a maximum of 10mm (EN1504-2) for effective performance.

Effective penetration depth can be defined as the depth of penetration from the surface of the treated concrete to the point where the untreated concrete starts (European standard EN 1504-2). It is determined by a method called the 'dip test'. Surface treated specimens are broken in half and the fractured surface/edge is exposed to water.

The untreated section of the fractured surface/edge will become dark from the wetting. Then penetration depth is measured from the surface of the treated edge to the region representing the untreated section (dark region due to wetting) on the fractured surface.

Lack of penetration into the substrate pore structure of hydrophobic treatments is one common problem that can be faced during application, this can be a result of evaporation of the product during application (volatility) or high localised humidity on the substrate surface or poor application method. Hence extreme care and caution should be exercised during the application process with consideration to the prescribed penetration depth.

#### *2.9.1.2 Type of surface treatment*

For practical purposes volatile products should be avoided in sunny and windy conditions as they pose a risk of evaporation during application. However, hydrophobic treatments (Silanes & Siloxanes) are polymers of varying carbon chain size giving rise to products with different volatility rate. Products with longer chains are less volatile and penetrate deeper than those with smaller chains (Selander, 2010).

Creamy products are common in hydrophobic treatments, since they offer easiness to apply evenly to surfaces without flowing and a distinguishable colour makes it easy to visualize

where further application is necessary. When spraying is used as an application method, the choice of equipment and pressure is very important, since high pressures can cause dissociation or separation of the product during application.

### 2.9.2 Coatings

#### *2.9.2.1 Application method*

The application methods of coatings to a substrate vary depending on the surface area or product type. Brushes, rollers, trowels or spray guns can be used for this purpose.

Each method has its advantages and disadvantages, for example rollers generally produce an uneven surface thickness. Thicker coatings can be difficult to apply with brushes, rollers or spray guns hence trowels can be used because of easy handling in this case. The moisture content and temperature of the substrate (concrete) should be appropriate as per product specification before application.

#### *2.9.2.2 Application temperature*

A temperature between 5 to 30°C is typically recommended and application should be avoided in rainy or moist conditions. However, cement based coatings can be applied during moist conditions. Most coatings are applied in several layers, with wet on wet application but others may require allowance for drying time between layers. Thickness after application is one of the critical parameter that affects the performance of the coating and should always be satisfied based on exposure conditions or product specification.

## 2.10 Results of Successful Surface Treatment Application

If correctly selected and applied, surface treatments can have a significant effect on the service life of reinforced concrete structures. Ingress of aggressive and essential elements that aids to deterioration of reinforcement can be minimised significantly when surface treatments are properly used.

Reduced moisture content inside the concrete due to surface treatments can result in increased carbon dioxide diffusion, and consequently carbonation rate, as illustrated in Figure 6. Hence it is important to select a surface treatment that suits the given environmental conditions of a specific site.

In the service life model of Figure 7, successful selection and application of surface treatments is represented by the grey line.

The service life, initiation and propagation period can be increased resulting in a longer period before maximum allowed corrosion has been reached.

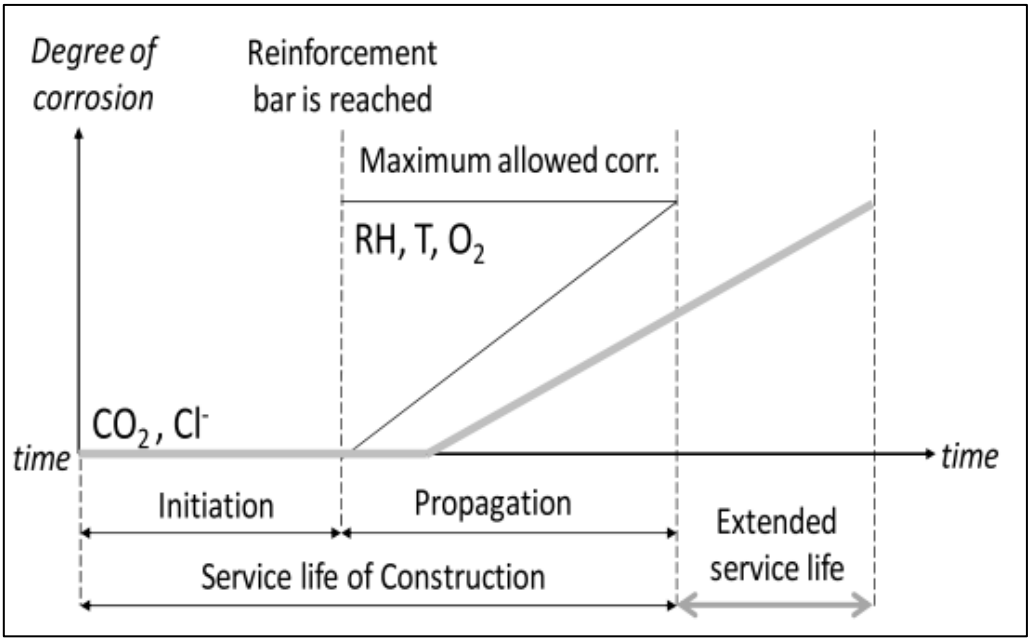


Figure 7: Resulting effect of surface treatments to the service life model of reinforced structures (Selander, 2010)

## 2.11 Conclusion

Surface treatments are not the answer to all the problems relating to durability of reinforced concrete via penetration by aggressive elements. However, if correctly applied, they can significantly impact and prolong the service life of a structure. The selection and application of surface treatment agents are dependent on many aspects ranging from exposure conditions to product and substrate type. Performance monitoring of surface treatment agents is also an integral aspect for successful results.

The protection mechanism of STAs span a wide range depending on the type of production. However their prime function is to avoid penetration of aggressive elements into the concrete by altering the concrete pore system or surface. This can be achieved by either blocking the pore system with precipitates, lining the surface pore system, or completely isolating the surface from external environment.

# 3 Corrosion Rate of Reinforcement in Concrete

## 3.1 Introduction

With time, the reinforcement embedded in concrete deteriorates when exposed to environments containing aggressive elements. The speed at which it corrodes is termed 'Corrosion Rate'. There are various techniques used to study the deterioration of reinforcement due to corrosion, varying from simple and less time consuming to complex and labour intensive methods, destructive and non-destructive methods. This research will focus on the most widely used non-destructive method to assess reinforcement corrosion; namely electrochemical technique.

## 3.2 Corrosion Rate Definition

Corrosion rate is a key parameter used to quantitatively predict the lifetime of structures under corrosion attack. It may inform about; the loss of cross-sectional area of reinforcing steel over time, and the time to cracking of concrete cover due to corrosion by products.

Andrade and Alonso formally define corrosion rate as; "*the amount of corrosion produced by a unit of surface area when referred to a specific period of time*" (Andrade & Alonso, 1996) . In simple terms corrosion rate is a parameter that can be measured as the loss of mass or weight of reinforcement due to corrosion over a period time.

## 3.3 Corrosion Rate Measurement Techniques

There are various electrochemical techniques that can be used to determine the corrosion intensity and subsequently corrosion rate of deteriorating reinforcement under attack by aggressive elements (e.g. chloride ions). Electrochemical techniques are based on the 'Linear Polarisation Resistance' of the reinforcement during the process of corrosion (Elsener, 1997).

The use of electrochemical methods to determine the corrosion rate or locating corroding areas has been a success story in the engineering field. However, the correct interpretation of electrochemical methods' data to corrosion risk or level is not as apparent as the methods. It is and has been a widely researched topic since the inception of electrochemical methods and various modifications and refinements have been done. This research study will focus

primarily on the use of a commercially available GECOR10 corrosion rate measuring instrument to assess the corrosion rate of reinforcement embedded in LWFC.

### 3.3.1 Linear polarization resistance methods

The method is attributed to Stern (Stern & Geary, 1957), the polarisation technique using direct current is one of the most widely used methods for corrosion rate monitoring. Stern used electrochemical fundamentals to propose a simple, fast and non-destructive technique.

The method encompasses a technique whereby the reinforcement (working electrode) is polarized by an external potential in the order of +/- 10mV relative to its open circuit potential (i.e. potential measured when no current is flowing in the reinforcement). As the potential of the reinforcement is changed, a current will be induced to flow between the working electrode and the counter electrode. The reinforcement's resistance to polarization is the gradient of the applied potential versus the induced current within the linear region of the potential versus current graph.

This approach of changing the potential of a metal in a sweep (controlled) manner and measuring the current induced is a technique called the Potentiostat method and the opposite of it, which is to apply a controlled current and measuring the potential induced, is called the Galvanostatic method. With both techniques, Potentiostat and Galvanostatic, a disturbance of the corrosion equilibrium process is initiated.

That is, the metal sample is forced from its open circuit potential and consequently referred to as being polarised and the response is measured as current. This response is used in modelling the corrosion behaviour of the reinforcement.

Expression 3.1 is known as the Stern's formula;

$$Rp = \left(\frac{\Delta E}{\Delta I}\right)_{\Delta E \to 0} \tag{3.1}$$

where: $Rp$ is the polarisation resistance, $\Delta E$ is the applied potential, and $\Delta I$ is the measured current.

The $Rp$ value is related to the corrosion current density ($Icorr$) or alternatively corrosion rate by means of a constant which Stern named $B$, and proposed a range of values for various

systems and states of corrosion. Using the proposed constants the $Icorr$ can be obtained by the equation:

$$Icorr = \frac{B}{Rp} \tag{3.2}$$

Where: $Icorr$ is the corrosion current density or corrosion rate, $B$ is Stern proposed constant (26mV for active corrosion and 52mV for passive corrosion), and $Rp$ is the polarisation resistance.

Stern's work was criticised for its simplicity, and during subsequent years researchers offered improvements which only increased the complexity without a clear improvement of the accuracy (Andrade & Alonso, 1996).

## 3.4 Electrochemical Basis of Corrosion

A corrosion process occurs via an electrochemical process involving two types of reactions, the anodic and cathodic reactions.

An anodic reaction is where metal oxidation occurs. Electrons are released into the metal. Corrosion products are formed are formed at the anodic region. Equation 3.3 represents the half-cell equation that takes place on the anodic region.

$$\mathrm{Fe} \rightarrow Fe^{2+} + 2e^{-} \tag{3.3}$$

Conversely, a cathodic reaction is where the reduction of the metal occurs. Electrons are removed from the metal reacting with water/moisture and oxygen forming hydroxyl ions which will migrate to the anodic region where they will form rust with $Fe^{2+}$ ions further initiating the reduction process on this region. Equation 3.4 represents the half-cell equation that takes place on the cathodic region.

$$4H_2O + O_2 + 2e^{-} \rightarrow 4OH^{-} \tag{3.4}$$

The equilibrium of the two above mentioned processes implies that there is a balanced flow of electrons from the anodic region the cathodic region. This equilibrium means that there is no current flow in the corroding metal.

To determine the corrosion current density ($Icorr$), which is related to the corrosion rate, the electrochemical techniques (Potentiostat or Galvanostatic methods) are implemented.

## *3.5* Theory behind Quantitative Measurement of Corrosion Data

The corrosion current density cannot be measured directly in a corroding reinforcement, electrochemical models are used to predict the value. The electrochemical methods assume that the anodic and cathodic process rates are controlled by the kinetics of the transfer reactions of ions and electrons on the metal surface during the corrosion process (ASTMG102, 1999; Berke & Brossia, 2005; Popov, 2015).

An electrochemical reaction which obeys the aforementioned assumption is represented by the equation below which is known as the Tafel equation.

$$I = I_o \, e^{\frac{2.303(E-E_o)}{\beta}} \tag{3.5}$$

Where $I$ is the current resulting from the electrochemical reactions presented by Equations 3.3 and 3.4, $I_o$ is a reaction dependent constant called the exchange current, $E$ is the electrode potential, $E_o$ is the equilibrium potential, and finally β is the Tafel constant.

Equation 3.5 represents an electrochemical behaviour in one isolated reaction (i.e. either anodic or cathodic reaction). But in a corrosion system two opposing reactions occur, which the behaviour is represented by the Butler-Volmer Equation 3.6:

$$I = I_{corr}\left( e^{\frac{2.303(E-E_{corr})}{\beta_a}} - e^{\frac{2.303(E-E_{corr})}{\beta_c}} \right) \tag{3.6}$$

Similar parameters of the Tafel and Butler equation mean the same except for: $I$ which now represents the measured current when using the Galvanostatic method (Section 3.4), $\beta_a$ and $\beta_c$ are anodic and cathodic Tafel constants respectively.

As mentioned previously, $Icorr$ values cannot be measured directly in a corroding system. Corrosion measurement instruments like the GECOR10 make use of software implementation that performs advanced numerical fit to the Butler-Volmer Equation 3.6, by adjusting the

measured values of potential ($E$), current ($I$) and the Tafel constants ($\beta_a$ & $\beta_c$) to obtain the $Icorr$ value.

## 3.6 Engineering Relationship to Electrochemical Data

As explained in (Section 3.5), the corrosion current density($Icorr$) is obtained by fitting the measured data (potential and current) in a corroding system to an electrochemical model (Butler-Volmer Equation 3.6).

To establish the corrosion rate in terms of an engineering parameter of mass loss over a period of time, the principal of Faraday's law is used (Bushman, 2002).

### 3.6.1 Faraday's law

During an electrolytic dissolution of a metal, say X, Equation 3.7 defines electrochemical process of dissolution:

$$X \rightarrow X^{n+} + n^{e-} \tag{3.7}$$

The relationship between current flow and mass loss is defined by the Faraday's law, equation 3.8:

$$Q = nFM \tag{3.8}$$

Where $Q$ is the charge resulting from the dissolution of a metal $X$ with units Coulombs, $n$ is the number of electrons that are transferred per mole of an atom of a metal $X$, $F$ is the Faraday's constant (96 485 Coulombs/mole), and $M$ is the number of moles of a metal $X$ reacting.

Charge, $Q$ is:

$$Q = I * t \tag{3.9}$$

Where $I$ is current flowing in the metal $X$ and, $t$ is time in seconds.

And number of moles, $M$ is:

$$M = \frac{m}{M_r} \tag{3.10}$$

Where $m$ is mass loss of a metal $X$ due to dissolution and $M_r$ is the molecular weight of a metal $X$. Substituting Equations 3.9 and 3.10 into Equation 3.8 ((Faraday's law) and rearranging we obtain the equation of mass loss of metal $X$ over time.

$$\frac{m}{t} = \frac{I\, M_r}{nF} \tag{3.11}$$

Equation 3.11 can be further simplified incorporating the metal $X$ density ($D$) to obtain an equation of volume loss over time. The volume loss over time is the same as the well know units of corrosion in engineering which is reinforcement depth corroded over time. Relating the current parameter ($I$) in Equation 3.11 to current density ($Icorr$), the parameter obtained by use of electrochemical techniques of reinforcement corrosion, the conversion constant from current density ($Icorr$) to uniform loss of reinforcement radius is given as:

$$\left(\frac{\text{mm}}{\text{year}}\right) = \frac{I_{corr} * M_r * t}{n * F * D} = \frac{I_{corr} 55.845 * 60 * 60 * 24 * 365}{2 * 96\,485\ * 7.874} = 0.0116 I_{corr} \tag{3.12}$$

(Andrade & Alonso, 1996; Jaske, Beavers, & Thompson, 2002; Miyazato & Hiraishi, 2013; RILEM TC 154-EMC, 2003).

Andrade & Alonso (1996) proposed a scale to classify the extent of corrosion in terms of $Icorr$ values. Figure 8 shows the $Icorr$ values as an indication of corrosion extent.

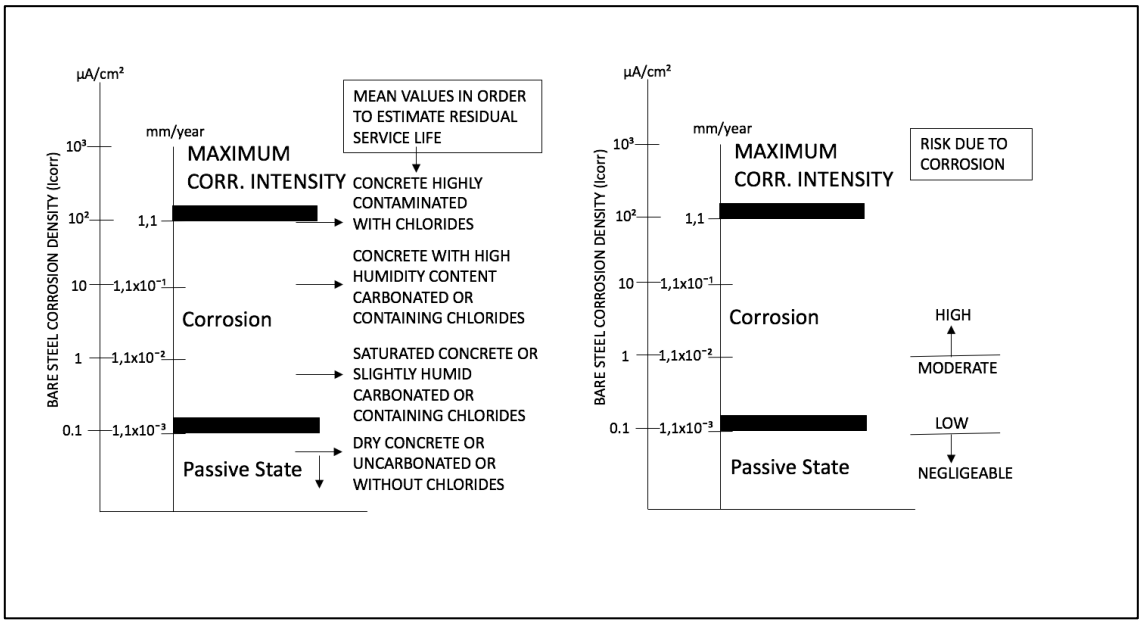


Figure 8: $I_{corr}$ values ranges for concrete under various conditions of humidity content and aggressive elements(Andrade & Alonso, 1996)

They classify the $Icorr$ values as follows; for $Icorr$ < 0.1 $\mu A/cm^2$ (1.1$\mu m/year$), the reinforcement is considered be under negligible corrosion, while for values above $Icorr$ > 0.2 $\mu A/cm^2$ (2.2$\mu m/year$), the reinforcement may be considered as undergoing corrosion.

Andrade & Alonso (1996) also provides the loss in rebar diameter prediction curves as a function of $Icorr$ and time. The rebar diameter loss graphs are applicable only when the corrosion process has reached the propagation period. Based on the time to reach a certain cross-sectional loss, the corrosion levels are established as negligible, low, moderate and high.

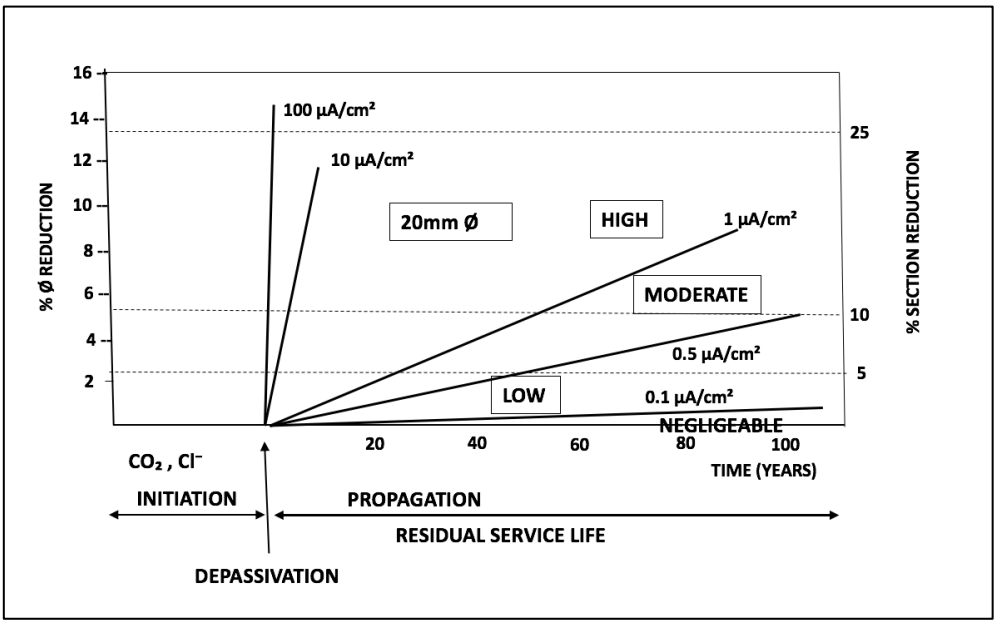


Figure 9: Decrease of rebar diameter/cross-section with time as a function of Icorr values during propagation period (Andrade & Alonso, 1996)

Rapid deterioration of the cross-section is indicated by values of $Icorr$ equating to 10 $\mu A/cm^2$. On the other hand, long life time of more than 100 years is suggested by values of $Icorr$ below 0.1 $\mu A/cm^2$.

Values suggesting a decrease in the cross-section by 5-25% during a service life period of 20-50 years are those having a rate of 0.5-5 $\mu A/cm^2$.

Based on the observations made by Andrade & Alonso (1996), Table 1 classifies the corrosion rate levels.

Table 1: Classification of corrosion level with reference to corrosion rate values (Andrade & Alonso 1996)

| Corrosion rate (μA/cm²) | Corrosion level |
|---|---|
| < 0.1 | negligible |
| 0.1 - 0.5 | low |
| 0.5 - 1 | moderate |
| > 1 | high |

Corrosion parameters are affected by temperature and moisture, hence it is difficult to formulate a universal interpretation system of the corrosion rate data. To account for the variation of corrosion parameters due temperature and moisture, literature provides some guidance for the interpretation of the corrosion monitoring results and classification based on the monitoring technique used (Martínez & Andrade, 2009). For the purposes of this study a linear polarization monitoring technique, as explained in Section 3.3.1 was used for determining the representative value of the corrosion rate in beam specimens.

# 4 Experimental Design

## 4.1 Introduction

This experimental design consisted of two main phases, material preparation and the testing phase. The LWFC material preparation will be presented first in this chapter and then followed by the detailed description of the tests conducted.

LWFC material and specimen preparation involves the selection of raw material, quantities determination, mixing procedure, casting specimens and then storage which will be covered in Sections 4.2 and 4.3. Section 4.4 will present the testing procedure, parameters tested and methods used.

## 4.2 Mix Design and Materials

A wet target density determines the strength category of LWFC, unlike in NWC where the required strength governs the water/cement ratio. A wet target density of 1600 kg/m$^3$ was established and used to determine the quantities of the mixing constituencies. This density was chosen as it falls within the structural category for LWFC (Alexander & Beushausen, 2009).

The materials presented in Section 4.2.1 were used to prepare the LWFC beams and cube specimens. For the purpose of this study, a target wet density of 1600 kg/m$^3$, foam density of 75 kg/m$^3$, water/cement ratio of 0.43, water/ash ratio of 0.25, and 0.45 percentage volume of fibres were kept constant throughout the preparation of LWFC.

### 4.2.1 LWFC materials

The main binder used to prepare the LWFC was Ordinary Portland Cement (CEM I) 52.5 N (SANS50197-1, 2013). A cement extender of Class S designated fly ash (SANS50450-1, 2014) under the brand name ULULA was also used.

The water used for both mixing and preparation of the pre-foam was potable water (SANS10100-2, 2014).A protein based foaming agent, with brand name Foamtech, was used to prepare the pre-foam. Synthetic polypropylene fibres (SAPY Corehfil™), 12mm in length, were incorporated in the preparation of all specimens.

## 4.3 Mixing Procedure and Test Specimens

### 4.3.1 Mixing procedure and quantities

The mix design in this research is based on the approach used by Kearsley & Mostert (2005). The authors used the hydraulic turntable test to determine the water demand of each mix design constituents. Appendix A gives in detail the procedure used by the authors and proposed equations to determine each constituent to satisfy the target density. Table 2 and Table 3 present the mixing contents used to prepare the three mix types of LWFC used in this study.

Table 2: Mix design constituents for the preparation of three types of LWFC

| Mix Type | | Density [kg/m³] | | | |
|---|---|---|---|---|---|
| | | Cement | Fly ash | Water | Foam |
| mix 1 | ash:cement = 0:1 | 1110 | 0 | 475 | 12.8 |
| mix 2 | ash:cement = 1:1 | 593.3 | 593.3 | 403.3 | 10.4 |
| mix 3 | ash:cement = 2:1 | 404.4 | 808.9 | 375.6 | 9.53 |

Table 3: Fibre properties

| Properties | Corehfil™ |
|---|---|
| material | 100% Virgin Polypropylene Homopolymer |
| fibre type | Straight Multifilament Fibre |
| density (g/cm³) | 0.91 |
| melting point (°C) | 160 |
| fibre diameter (µm) | 40 |
| fibre length (mm) | 12 |
| colour | Natural (white) |

The mixing procedure involved two stages which were as follows: a concrete mortar paste was separately prepared by mixing the dry aggregates and water.

A predetermined amount of foam was then added to the mortar paste and mixed again to make LWFC. Images of the LWFC drum mixer and the foam generating machine which were used in the production of LWFC are presented in Appendix A.

### 4.3.2 Test specimen preparation

Prismatic reinforced and unreinforced beam specimens with approximate dimensions of 460x100x100 mm and 500x100x100 mm respectively were cast for all the three mix designs (Table 2). A total of 24 reinforced and 12 unreinforced beam specimens were cast for each

mix design. The specimen distribution with regards to test parameters is detailed in Table 4. In addition to the beams, 100 mm cubes for mix design control on mixes 1, 2 and 3 were cast including specimens for long term compressive strength of mix design 3.

Table 4: Specimen sample size distribution per mix design

| cover | Specimen treatment | | |
|---|---|---|---|
| | Reference (REF) | impregnation (IT) | hydrophobic impregnation (ST) |
| 20 | 4 | 4 | 4 |
| 35 | 4 | 4 | 4 |
| Unreinforced | 4 | 4 | 4 |

Figure 10 shows the sectional views of the reinforced beams and the wooden shutter arrangements that were used to embed the reinforcement. In all the beam specimens (reinforced and unreinforced), a dike measuring 420x70 mm was cast-in on one longitudinal surface of the prismatic beams. The dike was used as a ponding pool to expose the beams to 0.3M NaCl concentrate solution.

Ribbed reinforcing steel bars of diameter Y12 mm at cover depths of 20 and 35 mm were used in the reinforced beam specimens (SANS920, 2011). The mass per unit length of the reinforcing bars is 0.888kg. The bars were cut as per shape code 20 (SANS282, 2011) and to an approximate length of 480 mm.

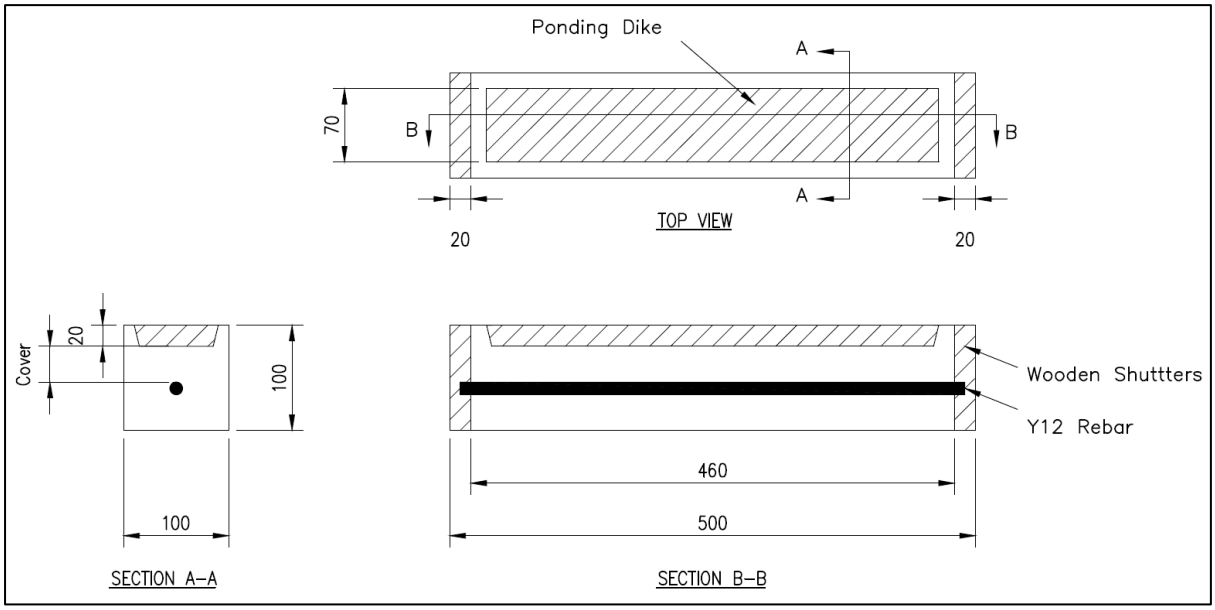


Figure 10: Reinforced beam specimen detail

Figure 11: Wooden mould

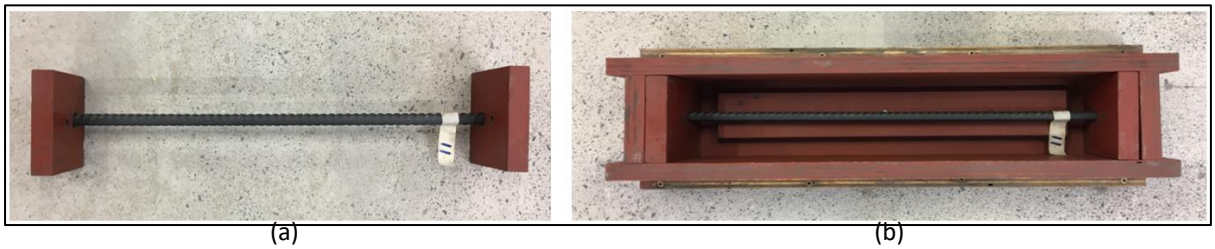

(a) (b)

Figure 12: (a) Rebar fixed to shatters (b) beam mould with rebar fixed to shutters assembly

The wooden mould in Figure 11 was used for casting both reinforced and unreinforced beam specimens.

For unreinforced specimens the mould without the reinforcement and shutter arrangement was used (Figure 11). For reinforced specimens the rebar was fixed onto the shutters as shown in Figure 12(a) and the shutters with the rebar were fixed into the mould as shown in Figure 12(b).

### 4.3.3 Specimen surface treating

Surface treatment on the specimens formed part of the test parameters. Two types of surface treatment agents were investigated, a waterproofing admixture for mortar and a silane based water repellent impregnation cream.

The waterproofing admixture was applied to the LWFC during the mixing stage to the impregnation (IT) set of the beam specimens for all three mix designs. The product used was a silicate-based agent (pore-blocker), brand name Sikalite®. The surface treatment was applied by mixing the powdery product mass of 0.2% by weight of the main binder with the dry mix constituents as specified by the product manufacturer (Sikalite®, 2012).

The brand name of the silane based water repellent (hydrophobic) impregnation cream used is Sikagard® – 706 Thixo and it is often referred to as the pore-liner in this study. It was applied onto the surface of the specimens after 28 days of curing by method of painting using a brush. The application method was also according to the manufacturer specification (Sikagard ® - 706 Thixo, 2012). Three coatings of the pore-liner agent were applied on the specimens' ponding dike. The specimens were then stored for 24 hours before testing to allow the treatment to penetrate the LWFC matrix.

Figure 13 shows two beam specimens after the final coat of treatment with a water repellent saline based agent (pore-liner).

Figure 13: Surface treated beam specimen by a saline-based agent (Sikagard® – 706 Thixo)

### 4.3.4 Specimen handling and storage

After casting specimens were stored for 24 hours in a climate controlled room with a relative humidity of 60±5 % and a temperature of 23±2 °C before demoulding (Figure 14). After the 24 hour period, when the LWFC had hardened, the moulds where stripped off and the beams were stored in the climate room for an additional curing period of 28 days before testing.

Figure 14: Cast beam specimens stored in the climate room to harden before demoulding

The cubes where also stored in the climate room to cure after demoulding and during the long term compressive strength testing.

## 4.4 Experimental Tests

### 4.4.1 Introduction

This section describes the experimental testing conducted in this study. The experimental tests were established in accordance with the objectives of the study. Performance of two types of surface treatment agents against chloride penetration and induced corrosion constituted the main focus of the study. In addition to that, long term compressive strength for a mix design with high fly ash inclusion was investigated. Sub-parameters investigated under chloride penetration and induced corrosion were; cement replacement with fly ash, and reinforcement cover depths of 20 and 35 mm respectively.

In order to investigate the surface treatment performance, fly ash content and cover depth; an accelerated laboratory cyclic wet/dry corrosion test was conducted. LWFC beam specimens were exposed to a wet period of NaCl solution and kept dry for the subsequent period after wetting.

### 4.4.2 Beams exposure to sodium chloride solution

After mixing, casting, curing and surface treating, the LWFC beam specimens were exposed to an aqueous solution of 0.3 M Sodium Chloride (NaCl) by means of ponding on the dike. The

NaCl solution was to induce chloride penetration and subsequent corrosion on the embedded reinforcement in the LWFC beams. Three repeated cycles, of 7 days ponding and 21 days dry, were performed to accelerate chloride ingress (i.e. 1 cycle = 7days wet and 21days dry).

The method of cyclic wetting and drying increases the concentration and penetration of chloride ions in the concrete matrix due to subsequent ingress and evaporation of water. During the dry period, oxygen availability in the concrete will be increased since it has a higher diffusion coefficient in unsaturated concrete.

In addition to increased oxygen penetration during the dry period, high degrees of dry period allows the subsequent wetting to carry chloride ions deeper into the concrete. The NaCl solution ponding and testing was conducted under climate-controlled conditions.

### 4.4.3 Parameters tested

The test parameters investigated in this study with regards to chloride penetration and induced corrosion were; surface treatment by a water repellent silane-based agent (pore-liner) and a silicate-based waterproofing admixture agent (pore-blocker) (i.e. surface treated; integrally treated; and reference untreated), fly ash content, with ash: cement ratios of 0:1, 1:1 and 2:1 (weight), and reinforcement cover depth of 20 mm and 35 mm.

In order to investigate the effect of the aforementioned parameters with regards to chloride penetration and induced corrosion in LWFC exposed to NaCl, a series of tests was conducted. Sections 4.4.3.1 to 4.4.3.3 present the details surrounding these tests. Information on the supplementary test, to determine the long term compressive strength development LWFC test specimens, is also included.

#### *4.4.3.1 Reinforcement corrosion rate*

There are various non-destructive testing techniques to assess corrosion rate of reinforcement embedded in concrete. For the purpose of this study the linear polarisation resistance (LPR) method using a commercially available GECOR 10 corrosion rate measuring equipment was implemented. The instrument has a built-in software that implements the LPR method based on the Potentiostat measurement technique (Andrade & Alonso, 1996; ASTMG102, 1999; Berke & Brossia, 2005; Gecor & Gecor, n.d.; Miyazato & Hiraishi, 2013).

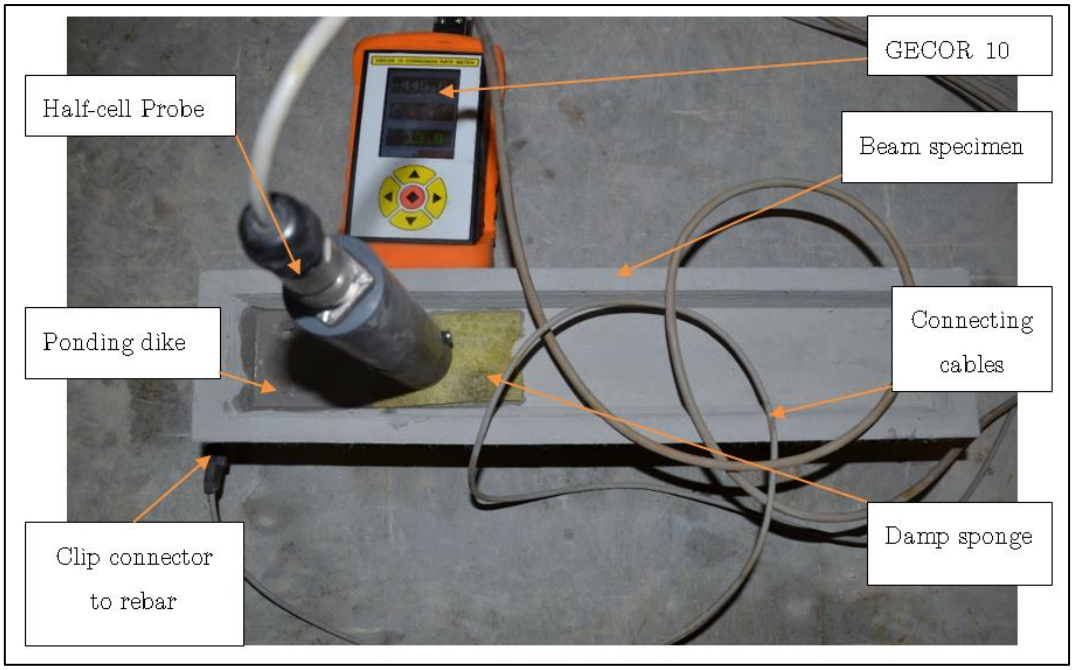


Figure 15: Typical reinforcement corrosion rate measurement set up

Figure 15 depicts the reinforcement corrosion rate measurement set up, accompanied by the GECOR 10 instrument, half-cell, and a beam specimen.

Reinforcement corrosion rate measurements for R/LWFC beams were recorded during the dry period. In the second and third cycle the readings were recorded at the end of the 21 days dry period. This decision was taken after a series of reinforcement corrosion readings in the first cycle proved to be influenced by the amount moisture saturation in the beam. Consistent and stable corrosion readings were observed to be recorded when the beam specimens are less saturated which was at the end of the 21 days dry period.

#### *4.4.3.2 Chloride penetration*

A total of nine unreinforced beam specimens were cut into half longitudinally with a saw blade after every cycle of exposure to determine the chloride penetration depth. The distribution of the nine beams was as follows: 3 beams per mix design for each treatment. A solution of 0.1 M silver nitrate concentration was sprayed over the cut surface and left for a few minutes so that the chemical reaction could take place.

The chloride ion penetration depth was measured using a Vernier callipers on the part that turned silver-white as a result of the chemical reaction between the silver nitrate and chloride

ions (Otsuki, Nagataki, & Nakashita, 1993). The maximum and minimum chloride ion penetration depths were recorded using this method.

The cut surfaces of all the beams were cleaned with pressurised air to remove the dust particles that might interfere with the chemical reaction when the silver nitrate is sprayed and consequently affect clear reading of the penetration depth results.

After air blowing, the surfaces were sprayed with the silver nitrate solution. The spraying technique was employed to avoid contamination of surfaces that had not been penetrated by chloride ions.

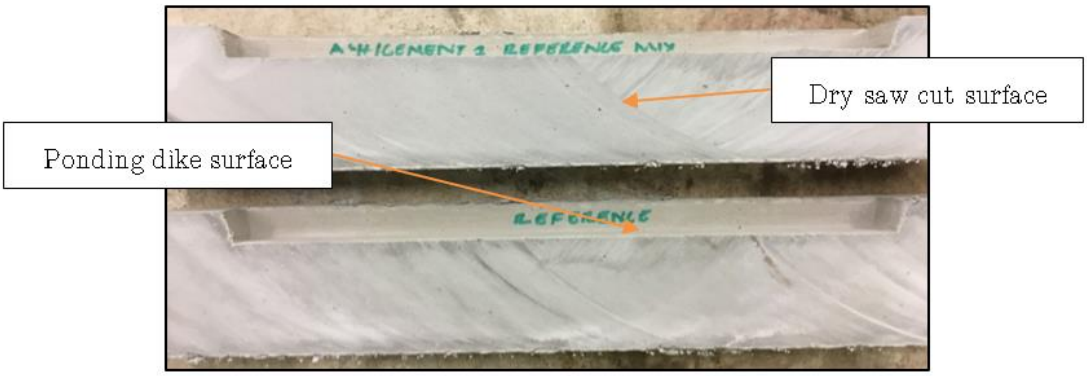


Figure 16: Cut unreinforced beam before spraying silver nitrate solution

The chloride penetration depth was defined as the distance from the bottom of the ponding dike to the lowest point with the silver-white discoloration. The test method was performed as explained and in accordance with the (ASTM C1543), the American standard test method for determining the penetration of chloride ion in concrete by ponding.

#### *4.4.3.3 Cube compressive strength*

In order to establish that the mix design satisfies the performance criteria of structural LWFC class based on strength; compressive strength testing was conducted as a mix design control test. It was performed in accordance to the South African National Standard (SANS5863, 2006). The test was conducted on 100 mm cube specimens at 28 days of aged. A Contest compressive strength testing machine type GD 10 grade A was used to determine the force to failure of the cube specimens. In addition a long term compressive test was also conducted

for mix design 3. This test was to further establish the consistency and validity of the mix design based on the strength prediction models for LWFC by Kearsley & Wainwright (2001). The long term compressive strength of mix design 3 cubes was determined at concrete age of 1, 3, 7, 14, 21, 28 and 56 days after casting. Equation 5.1 was used to calculate the compressive strength ($f_{cu}$)

$$f_{cu} = \frac{F_s}{A} \tag{5.1}$$

Where:

$F_s$: is the maximum force applied by a contest machine to a cube specimen

$A$: is the cross sectional area of the cube specimen normal to the applied force $F_s$

(SANS5863, 2006)

# 5 Experimental Results and Discussion

## 5.1 Introduction

This chapter presents the results obtained from the experimental tests conducted in the course of this research. The details and interpretation of the test results are also included.

The chloride penetration depth results are presented in Section 5.2, then followed by the crack characterisation in Section 5.3, Section 5.4 will present the corrosion rate results of the reinforcement bars embedded in the LWFC beams, and finally the cube compressive strength results in Section 5.5.

## 5.2 Chloride Penetration Results

Chloride penetration testing using silver nitrate solution was conducted to determine the ion penetration into unreinforced LWFC beams. This test was conducted to determine the penetration depth of chloride ions in the three LWFC mix designs prepared in this study. Figure 17 and Figure 18 depict the typical chloride penetration results at the end of NaCl ponding cycles 2 and 3.

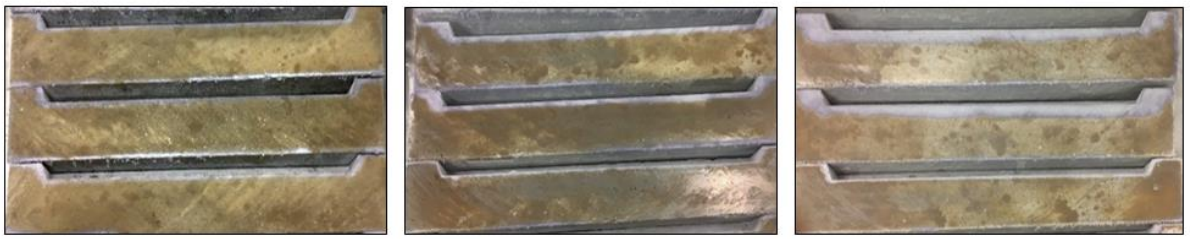

(a) (b) (c)

Figure 17: Typical silver nitrate discoloration of fly ash: cement ratio (a) 0:1, (b) 1:1, (c) 2:1 at the end of NaCl ponding cycle 2.

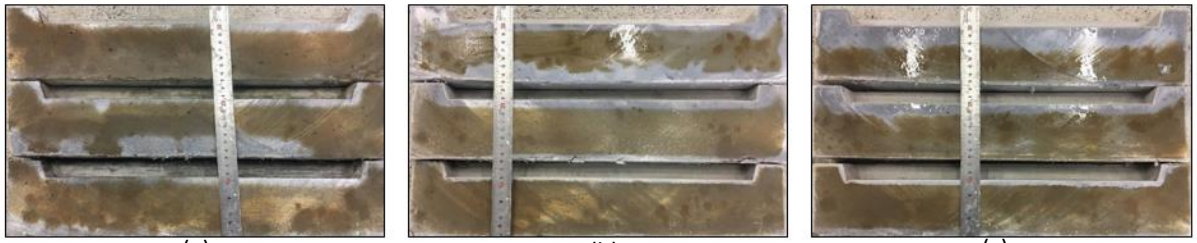

(a) (b) (c)

Figure 18: Typical silver nitrate discoloration of fly ash: cement ratio (a) 0:1, (b) 1:1, (c) 2:1 at the end of NaCl ponding cycle 3.

Table 5 gives the summary of the chloride penetration depths recorded via the silver nitrate chemical testing at the end of 1st, 2nd, and 3rd cyclic wetting and drying exposure cycles.

Table 5: Chloride penetration depth

| chloride penetration depth in [mm] | | | | | | | | | | |
|---|---|---|---|---|---|---|---|---|---|---|
| | | Reference (untreated/control) | | | Pore-blocker (integral) | | | Pore-liner (surface) | | |
| NaCl ponding cycles | | 1st | 2nd | 3rd | 1st | 2nd | 3rd | 1st | 2nd | 3rd |
| mix design 1 | ash:cement = 0:1 | 7 | 10 | 11 | 5 | 8 | 9 | 3 | 5 | 5 |
| mix design 2 | ash:cement = 1:1 | 9 | 11 | 12 | 8 | 10 | 12 | 3 | 5 | 5 |
| mix design 3 | ash:cement = 2:1 | 22 | 27 | 34 | 13 | 15 | 19 | 3 | 5 | 6 |

From Table 5, it can be deduced that the penetration depth is dependent on the type of surface treatment agent, fly ash content and period of NaCl exposure.

### 5.2.1 Surface treatment agent

Of the two surface treatment agents (pore-liner and pore-blocker) used in this study, the pore-liner (hydrophobic impregnation) agent exhibited a better performance against chloride ion penetration resistance. This behaviour can be attributed to the water repellent protection mechanism of the agent (Section 2.4.1.1). Concrete naturally forms ionic or hydrogen bonds with water molecules when in contact (hydrophilic state).

Upon application of the pore-liner agent, the concrete surface is altered from a hydrophilic state to a hydrophobic state which repels water molecules via a mechanism known as the lotus effect. The resulting hydrophobic surface is effective at resisting any form of moisture penetration into the concrete matrix, hence avoiding penetration by chloride ions in solution. The pore liner treatment agent proves to be effective on resisting any penetration by moisture, as depicted by the significantly small penetration depths in Table 5.

The pore blocker resists moisture penetration into the concrete matrix by reacting with the hydration products to form insoluble gel or precipitate that fills and blocks the easy movement of moisture in the concrete pore structure. However, the highly porous nature of LWFC is believed to have affected the effectiveness to penetration resistance of the agent. Since there will be significantly numerous pores to be blocked and that the protection mechanism of the agent results in a partially or totally filled capillaries or pores (EN1504-2).

A considerable penetration of moisture in the pore-blocker treated specimens, compared to the pore-liner treated specimens, was recorded.

### 5.2.2 Fly ash content

The penetration depth results in Table 5 show that an increase in fly ash content results in an increase in penetration of moisture in untreated LWFC beam specimens. Gao et al. (2009) mention that though high volumes of fly ash may reduce the shrinkage strains, the durability of concrete may be reduced at the same time. Replacement of Portland cement by fly ash is also reported to have an effect of increasing the porosity of a cement paste which may have compromised the durability against moisture penetration (P. Chindaprasirt, Homwuttiwong, & Sirivivatnanon, 2004). The pore-blocker treated specimens exhibited increase in penetration of moisture with increase in fly ash content, with doubled penetration depth between mix 1 and 3.

The moisture penetration resistance of the pore-liner treated specimens did not vary with increase in fly ash content. It can also be concluded that, increased periods of exposure to the NaCl cyclic wetting and drying, results in increased depth of chloride ion penetration.

## 5.3 Crack Characterisation

The presence of cracks on the reinforced beams had a significant impact on the trend of the corrosion rate profiles. The location along the beam that experienced cracks typically resulted in higher corrosion rate readings, this also applied for points closer to cracks. This section will present the crack characterisation of the reinforced specimens before presenting the corrosion profile results.

Dry shrinkage strains and restraint by the longitudinal beam resulted in multiple and random cracks being initiated as a way to relieve stress. The cracks varied from transverse to longitudinal. The location at which the cracks propagated did not follow any specific pattern rather than that of either being longitudinal, transversal or a combination of both. Figure 19 shows the typical crack pattern observed in the three mix designs.

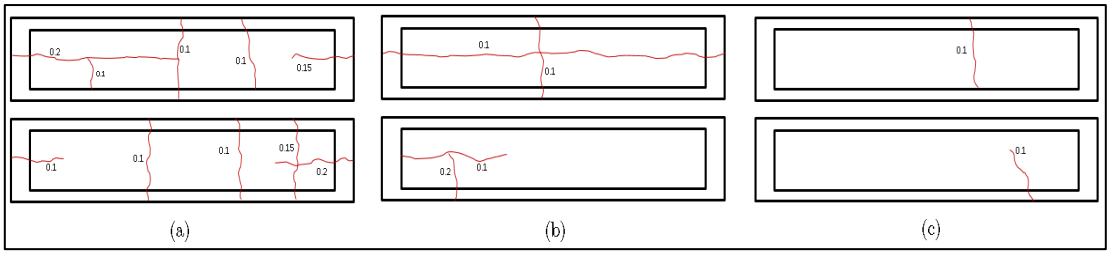


Figure 19: Typical cracks patterns (a) fly ash: cement ratio 0:1 (b) fly ash: cement ratio 1:1 (c) fly ash: cement ratio 2:2

As previously mentioned the propagation of cracks in the R/LWFC beams did not follow a specific trend or pattern. However with an increase in fly ash content the number of cracks and size reduced (Figure 19 (c)).

Figure 20 to Figure 22 present the crack distribution and size per set of beam specimens with regards to ash:cement ratio, and rebar cover.

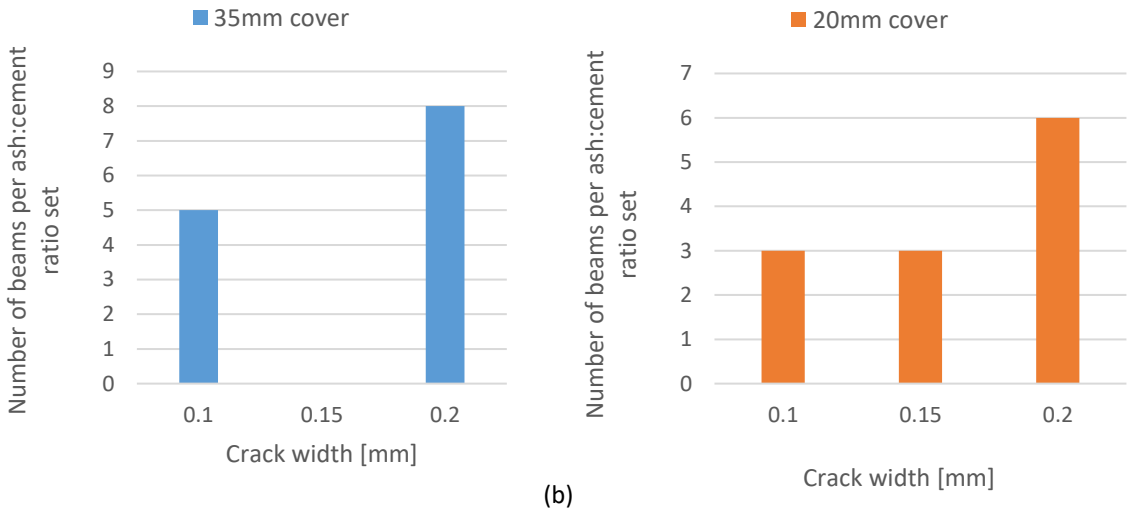


(a) (b)

Figure 20: Crack distribution in R/LWFC: ash/cement ratio 0:1 (a) 35mm cover (b) 20mm cover

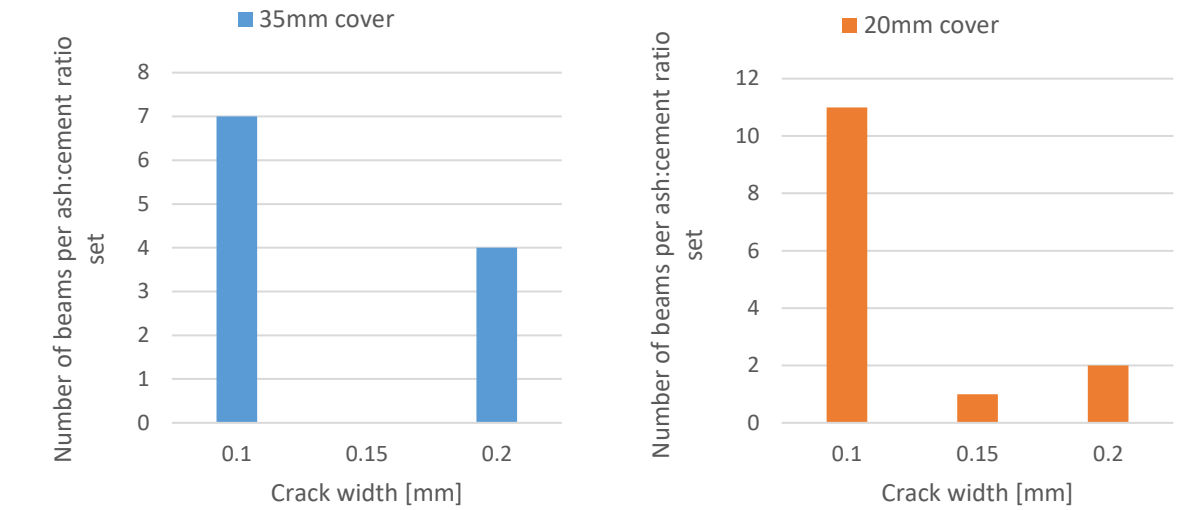


Figure 21: Crack distribution in R/LWFC: ash/cement ratio 1:1 (a) 35mm cover (b) 20mm cover

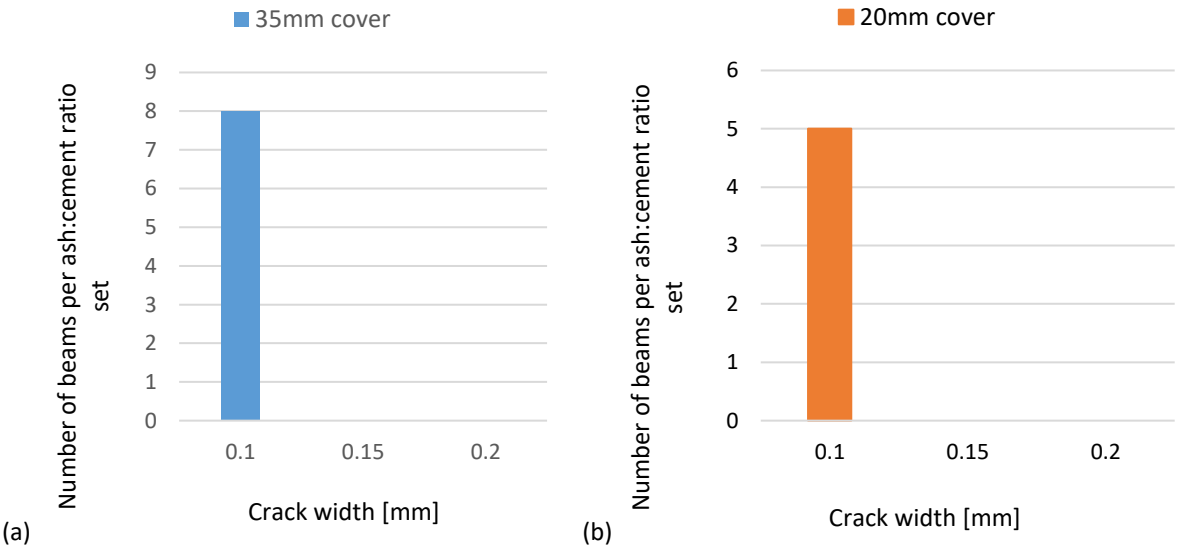


Figure 22: Crack distribution in R/LWFC: ash/cement ratio 2:1 (a) 35mm cover (b) 20mm cover

From Figure 20 to Figure 22 it can be deduced that the number of beams and crack size decreased with increase in fly ash:cement ratio. The crack distribution figures indicate that for a LWFC mix without fly ash inclusion (mix design 1), they were more beams with crack size greater than 0.2 mm. For mix design 2 and 3 the frequency of the beam crack size greater than 0.2mm reduces, with mix design 3 exhibiting a 0.1mm crack size distribution only.

Fly ash is well known for reducing the dry shrinkage strains in LWFC concrete, hence relieving the risk of cracking in restrained elements (Chindaprasirt & Rattanasak 2011; (P. Chindaprasirt et al., 2004; Prinya Chindaprasirt, Jaturapitakkul, & Sinsiri, 2005; Gao, Lu, & Tang, 2009) The properties of fly ash such as fineness and particle size can be attributed to the reduction of crack size with increase in fly ash: cement ratio depicted in Figure 20 to Figure 22.

Table 6: Corrosion rate characterisation with respect to crack size and distribution for ash:cement ratio 0:1

| Cover c [mm] | crack width $w_c$ [mm] | Nr. of cracks | Nr. of specimens | $I_{corr}$ [µA/cm²] | | |
|---|---|---|---|---|---|---|
| | | | | Avg. | Min | Max |
| 20 | 0.1 | 5 | 3: 2ST + 1REF | 1.34 | 1.08 | 1.53 |
| | 0.15 | 3 | 3: 2REF + 1IT | 5.13 | 2.11 | 7.38 |
| | 0.2 | 6 | 7: 2REF + 3ST + 2IT | 8.68 | 5.95 | 11.75 |
| 35 | 0.1 | 7 | 5: 3ST + 2IT | 3.83 | 1.84 | 4.35 |
| | 0.2 | 8 | 8: 3REF + 2ST + 3IT | 14.58 | 9.15 | 19.4 |

Table 7: Corrosion rate characterisation with respect to crack size and distribution for ash:cement ratio 1:1

| Cover c [mm] | crack width $w_c$ [mm] | Nr. of cracks | Nr. of specimens | $I_{corr}$ [µA/cm²] | | |
|---|---|---|---|---|---|---|
| | | | | Avg. | Min | Max |
| 20 | 0.1 | 12 | 8: 4REF + 2ST + 2IT | 1.28 | 0.11 | 3.11 |
| | 0.2 | 6 | 7: 3REF + 3ST + 2IT | 3.09 | 0.16 | 6.87 |
| 35 | 0.1 | 7 | 5: 1REF + 3ST + 1IT | 0.23 | 0.12 | 0.34 |
| | 0.2 | 4 | 4: 1REF + 2ST + 1IT | 0.34 | 0.24 | 0.42 |

Table 8: Corrosion rate characterisation with respect to crack size and distribution for ash:cement ratio 2:1

| cover c [mm] | crack width $w_c$ [mm] | Nr. of cracks | Nr. of specimens | $I_{corr}$ [µA/cm²] | | |
|---|---|---|---|---|---|---|
| | | | | Avg. | Min | Max |
| 20 | 0.1 | 5 | 4: 1REF + 3IT | 3.75 | 2.62 | 5.64 |
| 30 | 0.1 | 8 | 6: 1REF + 2ST + 3IT | 1.63 | 0.07 | 3.1 |

A summary of average, minimum and maximum values of corrosion rate for each crack size and distribution is presented in Table 6 to

Table 8. The corrosion rate values are irrespective of the surface treatment agent, however, they give a general perspective of the effect of crack size to corrosion rate. For each rebar cover an increase in the average corrosion rate is observed with increase in crack size. Significantly high corrosion rates were observed on cracked regions while recording the

corrosion profiles which signifies increased corrosion activity taking place at a crack and points surrounding it.

## 5.4 Corrosion Rate Profiles

This section analyses the performance of the surface treatment agents based on the corrosion rate of reinforcement embedded in LWFC.

The methods in determining the corrosion rate of embedded reinforcement in concrete cannot map the corrosion behaviour along the full length of the rebar. Yet the corrosion rate of rebar embedded in a beam can vary along the length of the bar as a result of the variable nature of material properties along the beam length.

The variations of the corrosion rate and material properties are due to factors such as; presence or absence of cracks in the beam; how far a point is from a crack; compaction is not perfectly homogenous along the beam length. In light of these factors, rebar corrosion rate profiles were produced by mapping the corrosion rate along the rebar length (rebar length corrosion mapping). This approach made it possible to visualise the effect of the aforementioned factors (especially cracking) on the corrosion rate of the reinforcement.

In order to visually assert a better performing surface protection system, the corrosion rate profiles were sorted based on mix design and rebar cover. Figure 23 to Figure 25 present the corrosion rate profiles obtained at the end of 2$^{nd}$ cycle of wetting and drying of R/LWFC beams. The corrosion rate data is presented in the form of current density (µA/cm$^2$) against rebar length (cm).

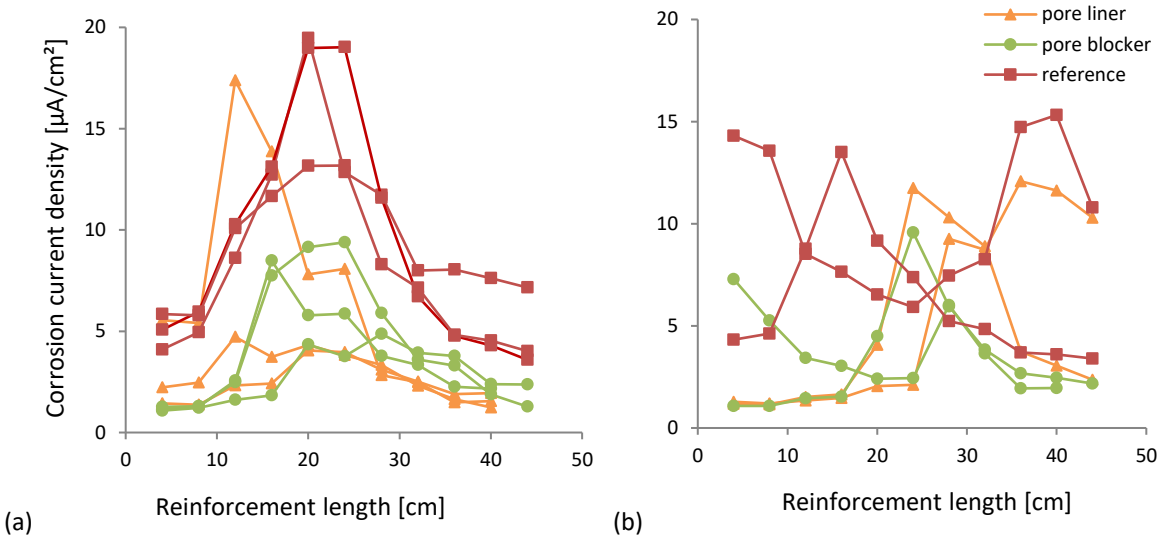


Figure 23: Corrosion current density for fly ash: cement ratio 0:1, for (a) 35 mm cover and (b) 20 mm cover

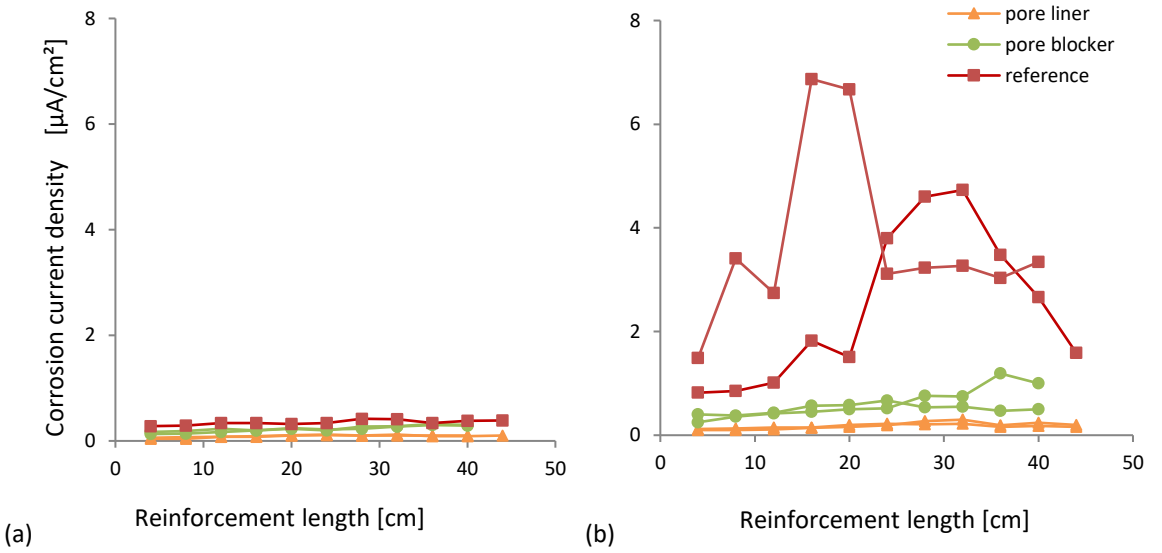


Figure 24: Corrosion current density for fly ash: cement ratio 1:1, for (a) 35 mm cover and (b) 20 mm cover

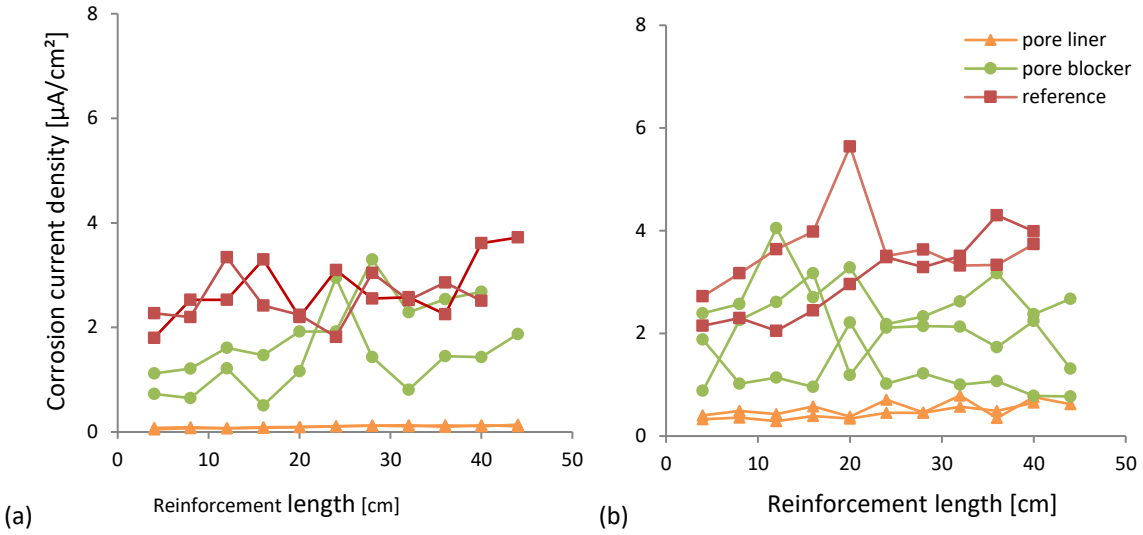


Figure 25: Corrosion current density for fly ash: cement ratio 2:1, for (a) 35 mm cover and (b) 20 mm cover

The corrosion behaviour of the reinforcement bars varied with content of fly ash inclusion in the mix design, and surface treatment agent.

### 5.4.1 Impact of fly ash inclusion on corrosion rate

LWFC is characterised by high drying shrinkage strain, making it susceptible to cracking in restrained elements (Awang, Mydin, & Roslan, 2012; Prinya Chindaprasirt & Rattanasak, 2011; Nambiar & Ramamurthy, 2008, 2009). The beam specimens without fly ash inclusion (Figure 23) experienced excessive longitudinal and transversal cracking as a result of drying shrinkage strain and reinforcement restraint. The cracks offered an easy pathway for the penetration of NaCl to the level of reinforcement.

The reference (untreated) specimens with a cover depth of 25mm developed longitudinal cracking at both ends of the beams (Figure 23 (b)), this can be seen by the increase in corrosion current rate profiles readings at the first and second end of the reinforcement.

With fly ash content increased the effects of drying shrinkage strain were observed to reduce, this was due to the reduction in crack width size and corrosion rate profiles readings recorded.

### 5.4.2 Impact of surface treatment agents on corrosion rate

Lower corrosion rates were recorded in surface treated pore-liner and pore-blocker specimens than in untreated specimens. However, it is difficult to distinguish or separate a

better treatment agent between the pore-blocker and the pore-liner agent from the corrosion profiles of mix design 1 specimens (fly ash: cement ratio 0:1). This is due to the excessive cracking as a result of dry shrinkage strains, rendering the surface treatment ineffective on resisting NaCl penetration.

Specimen cracking influenced the corrosion rate profiles trend for the LWFC mix design 1 without fly ash inclusion (Figure 23). A similar trend of the corrosion rate profiles is observed regardless of the applied surface treatment or rebar cover depth. Though cracks were dominant, surface treatments arguably offer some level of protection for mix design 1 specimens which can be observed at both ends of the rebar corrosion profile (Figure 23).

The effects of cracks reduce with fly ash inclusion in mix designs 2 and 3, which correspond to corrosion rate profiles in Figure 24 and Figure 25. The corrosion profiles in mixes with fly ash inclusion were not affected by shrinkage strains to a significant extent, this made it possible to qualitatively asses the effectiveness of surface treatment agents. The pore-liner agent can be regarded as better performing than the pore-blocker. This can be supported by observed lower corrosion current rate profile readings for the pore liner system in Figure 24 and Figure 25. The corrosion profiles at the end of the 3rd NaCl exposure cycle are presented in Figure 26 to Figure 28.

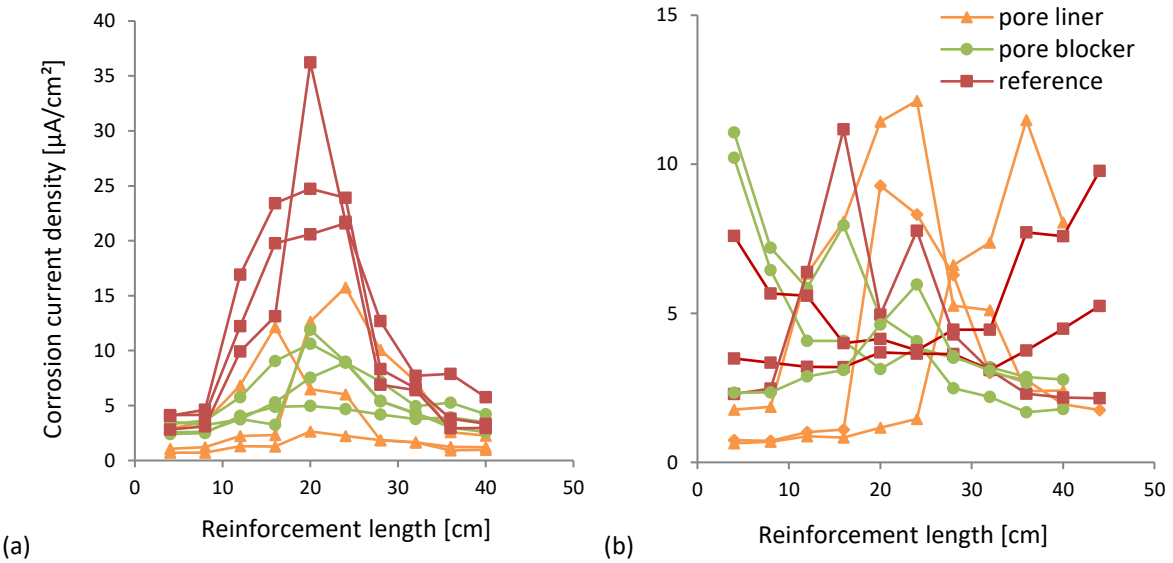


Figure 26: Corrosion current density for fly ash: cement ratio 0:1, for (a) 35 mm cover and (b) 20 mm cover

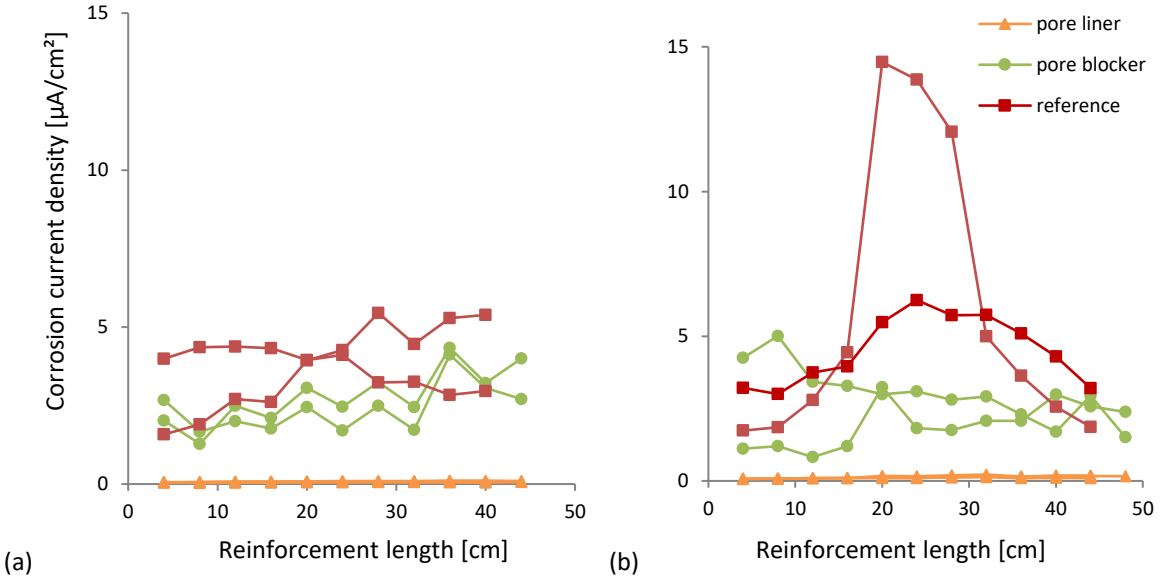


Figure 27: Corrosion current density for fly ash: cement ratio 1:1, for (a) 35mm cover and (b) 20mm cover

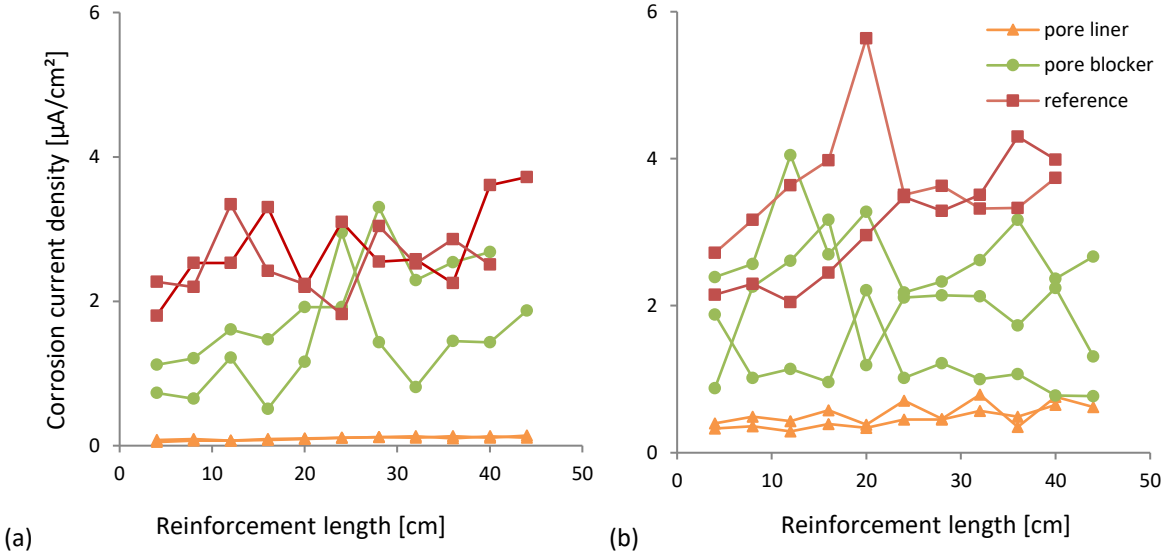


Figure 28: Corrosion current density for fly ash: cement ratio 2:1, for (a) 35 mm cover and (b) 20 mm cover

An increase of the corrosion rate profile readings is observed between the profiles recorded during the 2nd and 3rd exposure cycle. However a consistent trend for both cycles is apparent. The increase in corrosion rate profiles readings in the 3rd cycle data is due to the subsequent NaCl solution ponding, which adds to the already occurring corrosion process.

A qualitative analysis of the corrosion profiles of the 2nd and 3rd exposure cycles shows that the pore-liner treated specimens offered better performance at inhibiting chloride induced corrosion. This observation agrees with the conclusions made by Vries (1997) on the study pertaining to hydrophobic treatment of concrete.

## 5.5 Compressive Strength Results

The compressive strength test was performed mainly as a mix design control. The crushed specimen results were compared to the results obtained from the prediction models, Equations 5.1, 5.2 and 5.3 as proposed in literature by Kearsley and Wainwright.

$$p = 18665 y_d^{-0.8440} \quad (5.1)$$

$$f_p = 39.6(\ln(t))^{1.174}(1-p)^{3.60} \quad (5.2)$$

$$f_{fc} = 1.172 f_p \alpha_b^{3.70} \quad (5.3)$$

(Kearsley & Wainwright, 2001b)

Where: $p$ = porosity (%); $y_d$ = dry density (kg/m$^3$); $f_p$= cube compressive strength of paste (MPa); $t$ = time since casting/concrete age (days); $f_{fc}$= compressive strength of foamed concrete (MPa); $\alpha_b$ = binder ratio.

Binder ratio is all the binder contents (by volume) including mixing water of foamed concrete mixture expressed as a fraction of all the binder content of the cement paste (base mix).

The typical 28 day strength of LWFC with ash: cement ration of 2:1 was found to give an average of 19MPa. Fly ash replacement in LWFC resulted in low early age strength development as expected, however the strength development gradually increased with time.

According to the models the age at which the strength parity between the ash: cement ratio 0:1 mix and the two ash: cement ratio 1:1 and 2:1 mixes was 125 days and 171 days respectively. However the models for the mixes with fly ash inclusion predicted an overall higher long term strength development. This may be due to the pozzolanic reaction of fly ash's alumina-silicate with the Portland cement hydration product calcium hydroxide to produce various calcium-silicate hydrates and calcium-aluminate hydrates which adds to strength development of the LWFC.

Long term compressive strength test for ash: cement ratio 2:1 results, including the prediction models, are presented in Figure 29. The long term compressive strength test was conducted in order to establish a mix design control criteria for the mix with high fly ash content. An agreement of the test results and the prediction models can be observed.

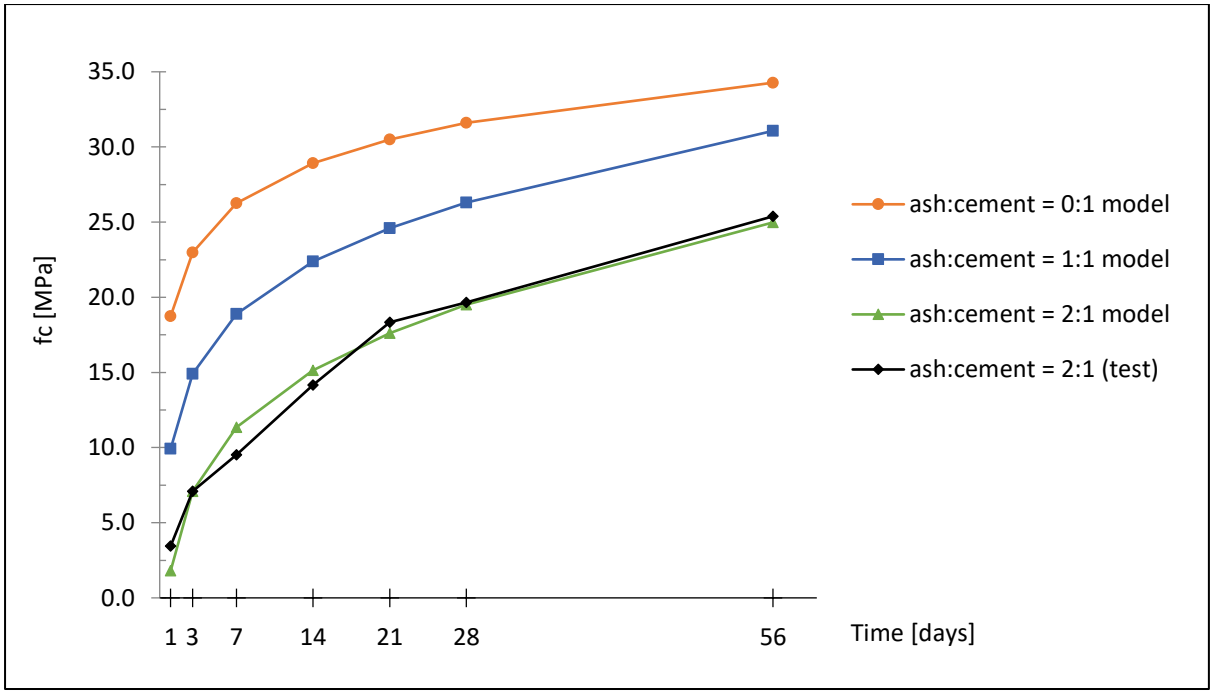


Figure 29: Long-term strength development of LWFC

# 6 Conclusion and Recommendations

## 6.1 Introduction

The research investigated the performance of two locally sourced (South African) surface treatment agents against resisting chloride penetration and consequently induced corrosion in LWFC. The chloride induced corrosion was initiated by means of cyclic wetting and drying of beam specimens with NaCl solution. Three types of LWFC mixes with fly ash inclusion of ash: cement ratios of 0:1, 1:1 and 2:1 were prepared for testing. The chloride penetration depth and corrosion rate of embedded reinforcement were recorded at the end of each NaCl ponding cycle which consisted of 7 days wet and 21 days dry equating to 1 cycle, and a total of 3 cycles were performed.

The results from the tests conducted indicated that the performance of surface treatment agents can be compromised by the presence of cracks in the specimens. This observation was confirmed by the variance of the corrosion rate profiles from severely cracked to un-cracked specimens. The conclusion can be summarised as follows:

## 6.2 Conclusions

### 6.2.1 Lightweight foamed concrete (LWFC)

- LWFC without cement extenders (fly ash) offers an appreciable resistance to moisture penetration. However, high dry shrinkage strains, which give a high risk of cracking in restrained elements or members of the material, are a major concern that needs attention in order to enhance the durability performance of the material.

### 6.2.2 Surface treatment agents

- The analysis of the corrosion rate and chloride penetration depth results shows that the saline-based treatment agent (pore-liner) performed better than the silicate-based treatment agent (pore-blocker) in preventing chloride ion penetration in solution and consequently limiting the rate of corrosion.

### 6.2.3 Fly ash content

- Fly ash inclusion in the LWFC mix yielded positive results against the effects of dry shrinkage strain in restrained LWFC elements, which are prone to risk of heavy cracking.
- From the mix design constituents in Table 2, it can be drawn that fly ash has a positive effect on reducing the water demand of a mix. With increase in fly ash content, the

water requirements of the mix design decreased. Fly ash requires less water owing to its spherical shape and smooth surface.

- Chloride ion penetration depth was observed to increase with increase in fly ash content for the untreated specimens, the effect of which compromises the durability properties of LWFC with high fly ash content hence the content of fly ash needs to be controlled.
- From the three mix designs investigated in this study, the mix design with equal proportions of fly ash and cement content ( ash: cement ratio 1:1) can be considered to be the better performing mix with regards to chloride penetration, dry shrinkage cracking and chloride induced corrosion of embedded rebar. This indicates that the cost of LWFC mixture can be reduced by replacing an equal amount of cement with fly ash without compromising the durability performance of the concrete.
- With regards to compressive strength, a low rate of early age strength development is observed for LWFC mix with high fly ash inclusion (ash: cement ratio 2:1). However a gradual increase in strength can be observed which is attributed to the pozzolanic effect of fly ash in concrete.

## 6.3 Recommendations

Durability enhancement of LWFC by use of surface treatment agents for application in reinforced elements or members exposed to aggressive elements can be achieved successfully. However, this study did not include other factors that affect durability such as effects of exposure to the natural environment. Hence, based on the work conducted in this research, the following recommendations can be considered for further studies:

- Tests to investigate the impact of natural environmental factors on the performance of surface treatment agents.
- Further study on the shrinkage behaviour of LWFC with and without fly ash inclusion, and with focus on but not limited to the material's plastic, autogenous and dry shrinkage behaviour to quantify the effect of fly ash replacement.
- Further study to investigate the performance of other types of surface treatment agents and combinations of two or more agents can be explored.
- The application and performance of shrinkage-reducing admixtures (SRAs) can also be an area of interest for further study towards mitigating crack propagation in restrained LWFC elements.
- Investigation of a wide range of fly ash to cement ratio proportions in LWFC with respect to durability performance to ascertain the optimum and maximum quantities of fly ash that can be included in the mixing constitutes without compromising the durability properties and capabilities of the material.

# 7 Reference List

Aguiar, J. B., & Junior, C. (2013). Carbonation of surface protected concrete. *Construction and Building Materials*, *49*, 478–483. https://doi.org/10.1016/j.conbuildmat.2013.08.058

Alexander, M., & Beushausen, H. (2009). *Deformation and volume change of hardened concrete*. *Fulton's Concrete Technology*.

Andrade, C., & Alonso, C. (1996). Corrosion rate monitoring in the laboratory and on-site. *Construction and Building Materials*, *10*(5 SPEC. ISS.), 315–328. https://doi.org/10.1016/0950-0618(95)00044-5

ASTMG102. (1999). Standard Practice for Calculation of Corrosion Rates and Related Information. *Astm G 102*, *89*(Reapproved), 1–7. https://doi.org/10.1520/G0102-89R10

Awang, H., Mydin, M. A. O., & Roslan, A. F. (2012). Effects of Fibre on Drying Shrinkage, Compressive and Flexural Strength of Lightweight Foamed Concrete. *Advanced Materials Research*, *587*(December), 144–149. https://doi.org/10.4028/www.scientific.net/AMR.587.144

Bach, F. W., Bormann, D., Kucharski, R., & Wilk, P. (2004). Production and Properties of Foamed Magnesium. *Cellular Metals and Polymers*, (April), 1–4.

Basheer, P. A. M., Basheer, L., Cleland, D. J., & Long, A. E. (1997). Surface treatments for concrete: assessment methods and reported performance. *Construction and Building Materials*, *11*, 413–429. https://doi.org/10.1016/S0950-0618(97)00019-6

Berke, N. S., & Brossia, S. (2005). Electrochemical Techniques for Corrosion Monitoring and Maintenance. In H. Böhni (Ed.), *Corrosion in reinforced concrete structures* (pp. 215–240). Cambridge, England: Woodhead. Retrieved from https://books.google.co.za/books?hl=en&lr=&id=3Y-pAgAAQBAJ&oi=fnd&pg=PP1&dq=Corrosion+in+Reinforced+Concrete+Structures&ots=yCfn5_RMwq&sig=q9WX7qUCf-BIcwoZARJUSGSTVvI#v=onepage&q=Corrosion in Reinforced Concrete Structures&f=false

Böhni, H. (2005). *Corrosion in reinforced concrete structures*. Woodhead. Retrieved from https://books.google.co.za/books?hl=en&lr=&id=3Y-pAgAAQBAJ&oi=fnd&pg=PP1&dq=Corrosion+in+Reinforced+Concrete+Structures&ots=yCfn5_RMwq&sig=q9WX7qUCf-BIcwoZARJUSGSTVvI#v=onepage&q=Corrosion in Reinforced Concrete Structures&f=false

Brady, K. C., Brady, K. C., Watts, G. R. A., Jones, I. R., Brady, K. C., Watts, G. R. A., & Jones, M. R. (2001). SPECIFICATION FOR FOAMED CONCRETE. Retrieved from http://citeseerx.ist.psu.edu/viewdoc/summary?doi=10.1.1.695.3794

Bushman, J. B. (2002). Calculation of Corrosion Rate from Corrosion Current ( Faraday ' s Law ) by. *Corrosion*, 7–10. Retrieved from www.bushman.cc/pdf/faradays_law.pdf

Chindaprasirt, P., Homwuttiwong, S., & Sirivivatnanon, V. (2004). Influence of fly ash fineness on strength, drying shrinkage and sulfate resistance of blended cement mortar. *Cement and Concrete Research*, *34*(7), 1087–1092. https://doi.org/10.1016/j.cemconres.2003.11.021

Chindaprasirt, P., Jaturapitakkul, C., & Sinsiri, T. (2005). Effect of fly ash fineness on compressive strength and pore size of blended cement paste. *Cement and Concrete Composites*, *27*(4), 425–428. https://doi.org/10.1016/j.cemconcomp.2004.07.003

Chindaprasirt, P., & Rattanasak, U. (2011). Shrinkage behavior of structural foam lightweight concrete containing glycol compounds and fly ash. *Materials and Design*, *32*(2), 723–727. https://doi.org/10.1016/j.matdes.2010.07.036

De Villiers, J., Van Zijl, G., & van Rooyen, A. (2016). Fracture of lightweight foamed concrete in evaluation of bond behaviour of steel reinforcement embedded in LWFC. *Proceedings of the 9th International Conference on Fracture Mechanics of Concrete and Concrete Structures*. https://doi.org/10.21012/FC9.289

Elsener, B. (1997). Corrosion Rate of Steel in Concrete - From Laboratory to Reinforced Structures. *Materials Science Forum*, *247*, 127–138. https://doi.org/10.4028/www.scientific.net/MSF.247.127

Franzoni, E., Pigino, B., & Pistolesi, C. (2013). Ethyl silicate for surface protection of concrete:

Performance in comparison with other inorganic surface treatments. *Cement and Concrete Composites*, *44*, 69–76. https://doi.org/10.1016/j.cemconcomp.2013.05.008

Fridh, K. (2005). *Internal frost damage in concrete : experimental studies of destruction mechanisms*. Lund Institute of Technology. Retrieved from http://portal.research.lu.se/portal/en/publications/internal-frost-damage-in-concrete--experimental-studies-of-destruction-mechanisms(4de14db9-9e4c-44d6-8fb2-067fe280e6a2).html

Gao, P., Lu, X., & Tang, M. (2009). Shrinkage and expansive strain of concrete with fly ash and expansive agent. *Journal Wuhan University of Technology, Materials Science Edition*, *24*(1), 150–153. https://doi.org/10.1007/s11595-009-1150-4

Gecor, E., & Gecor, N. (n.d.). GECOR-10.

Giessler, S., Standke, B., & Büchler, M. (2005). A new silane system for corrosion reduction of steel reinforced concrete. *Hydrophobe IV: Fourth International Conference on Water Repellent Treatment of Building Materials*, *26*, 17–26.

Hazlin, A. R., Iman, A., Mohamad, N., Goh, W. I., Sia, L. M., Samad, A. A. A., & Ali, N. (2017). Microstructure and Tensile Strength of Foamed Concrete with Added Polypropylene Fibers. *MATEC Web of Conferences*, *103*(April), 1013. https://doi.org/10.1051/matecconf/201710301013

Jaske, C. E., Beavers, J. A., & Thompson, N. G. (2002). Improving plant reliability through corrosion monitoring. *Corrosion Prevention and Control*, *49*(1), 3–12. Retrieved from http://www.scopus.com/inward/record.url?eid=2-s2.0-0036504615&partnerID=tZOtx3y1

Jia, L., Shi, C., Pan, X., Zhang, J., & Wu, L. (2016). Effects of inorganic surface treatment on water permeability of cement-based materials. *Cement and Concrete Composites*, *67*(January), 85–92. https://doi.org/10.1016/j.cemconcomp.2016.01.002

Johansson Janz, M., Silfwerbrand, J., Trägårdh, J., A. (2005). Protection of concrete with water repellent agents – What is required to achieve a sufficient penetration depth? *Hydrophobe IV 4. International Conference on Water Repellent Treatment of Building*

*Materials*, (Taylor & Francis Group, London, ISBN 978-0-415-46850-3 Aedificatio Publishers), 133–144. https://doi.org/10.1201/9781439828403.ch105

Jones, M. R., & McCarthy, A. (2005). Preliminary views on the potential of foamed concrete as a structural material. *Magazine of Concrete Research*, *57*(1), 21–31. https://doi.org/10.1680/macr.2005.57.1.21

Kearsley, E. P., & Wainwright, P. J. (2001a). Porosity and permeability of foamed concrete. *Cement and Concrete Research*, *31*(5), 805–812. https://doi.org/10.1016/S0008-8846(01)00490-2

Kearsley, E. P., & Wainwright, P. J. (2001b). The effect of high fly ash content on the compressive strength of foamed concrete. *Cement and Concrete Research*, *31*(1), 105–112. https://doi.org/10.1016/S0008-8846(00)00430-0

Martínez, I., & Andrade, C. (2009). Examples of reinforcement corrosion monitoring by embedded sensors in concrete structures. *Cement and Concrete Composites*, *31*(8), 545–554. https://doi.org/10.1016/j.cemconcomp.2009.05.007

Medeiros, M. H. F., Aleixo, D. M., Quarcioni, V. A., Marcondes, C. G. N., Helene, P., Prado, A. A., & Prado, A. (2012). Reducing Water and Chloride Penetration Through Silicate Treatments for Concrete as a Mean to Control Corrosion Kinetics. *Construction and Building Materials*, *7*, 9682–9696.

Medeiros, M. H. F., & Helene, P. (2009). Surface treatment of reinforced concrete in marine environment: Influence on chloride diffusion coefficient and capillary water absorption. *Construction and Building Materials*, *23*(3), 1476–1484. https://doi.org/10.1016/j.conbuildmat.2008.06.013

Miyazato, S., & Hiraishi, Y. (2013). Durability against Steel Corrosion of HPFRCC with Bending Cracks. *Journal of Advanced Concrete Technology*, *11*(4), 135–143. https://doi.org/10.3151/jact.11.135

Nambiar, E. K. K., & Ramamurthy, K. (2008). Fresh State Characteristics of Foam Concrete. *Journal of Materials in Civil Engineering*, *20*(2), 111–117. https://doi.org/10.1061/(ASCE)0899-1561(2008)20:2(111)

Nambiar, E. K. K., & Ramamurthy, K. (2009). Shrinkage Behavior of Foam Concrete. *Journal of Materials in Civil Engineering*, *21*(11), 631–636. https://doi.org/10.1061/(ASCE)0899-1561(2009)21:11(631)

Neville, A. (1995). Chloride Attack of Reinforcement Conccrete an Overview.Pdf. *Materials and Structures*. https://doi.org/10.14359/10569

Otieno, M. (2010). Transport mechanisms in concrete. Corrosion of steel in concrete (initiation, propagation & factors affecting). *University of Cape Town*, 83. Retrieved from http://scholar.google.com/scholar?hl=en&btnG=Search&q=intitle:Transport+mechanisms+in+concrete:+Corrosion+of+steel+in+concrete+-+Initiation,+propagation+&+factors+affecting#1

Otsuki, N., Nagataki, S., & Nakashita, K. (1993). Evaluation of the AgNO3 solution spray method for measurement of chloride penetration into hardened cementitious matrix materials. *Construction and Building Materials*, *7*(4), 195–201. https://doi.org/10.1016/0950-0618(93)90002-T

Panesar, D. K. (2013). Cellular concrete properties and the effect of synthetic and protein foaming agents. *Construction and Building Materials*, *44*, 575–584. https://doi.org/10.1016/j.conbuildmat.2013.03.024

Pigino, B., Leemann, A., Franzoni, E., & Lura, P. (2012). Ethyl silicate for surface treatment of concrete - Part II: Characteristics and performance. *Cement and Concrete Composites*, *34*(3), 313–321. https://doi.org/10.1016/j.cemconcomp.2011.11.021

Popov, B. N. (2015). Electrochemical Kinetics of Corrosion. In *Corrosion Engineering* (pp. 93–142). Elsevier. https://doi.org/10.1016/B978-0-444-62722-3.00003-3

Raupach, M., & RÖßLER, G. (2005). Surface treatments and coatings for corrosion protection. In H. Böhni (Ed.), *Corrosion in reinforced concrete structures* (pp. 163–189). Cambridge, England: Woodhead. Retrieved from https://books.google.co.za/books?hl=en&lr=&id=3Y-pAgAAQBAJ&oi=fnd&pg=PP1&dq=Corrosion+in+Reinforced+Concrete+Structures&ots=

yCfn5_RMwq&sig=q9WX7qUCf-BIcwoZARJUSGSTVvI#v=onepage&q=Corrosion in Reinforced Concrete Structures&f=false

RILEM TC 154-EMC. (2003). Recommendations of RILEM TC 154-EMC: "Electrochemical Techniques for Measuring Metallic Corrosion"- Half-cell potential measurements-Potential mapping on reinforced concrete structures. *Materials and Structures*, *36*(September), 461–471. https://doi.org/10.1007/BF02481526

Sandrolini, F., Franzoni, E., Pigino, B., Dai, J. G., Akira, Y., Wittmann, F. H., … Wainwright, P. J. (2012). Ethyl silicate for surface treatment of concrete - Part I: Pozzolanic effect of ethyl silicate. *Cement and Concrete Composites*, *34*(3), 306–312. https://doi.org/10.1016/j.cemconcomp.2011.12.003

SANS10100-2. (2014). *SANS 10100-2 : 2014 SOUTH AFRICAN NATIONAL STANDARD - The structural use of concrete, Part 2: Materials and execution of work* (3rd ed.). Pretoria, South Africa: SABS Standards Division.

SANS282. (2011). *SANS 282 : 2011 SOUTH AFRICAN NATIONAL STANDARD Bending dimensions and scheduling of steel reinforcement for concrete* (6th ed.). Pretoria, South Africa: SABS Standards Division.

SANS50197-1. (2013). *SANS 50197-1 : 2013 South African National Standard Cement Part 1: Composition , specifications and conformity criteria for common cements* (2nd ed.). Pretoria, South Africa: SABS Standards Division.

SANS50450-1. (2014). *SANS 50450-1 : 2014 SOUTH AFRICAN NATIONAL STANDARD Fly ash for concrete Part 1 : Definition , specifications and conformity criteria* (2nd ed.). Pretoria, South Africa: SABS Standards Division.

SANS5863. (2006). *SANS 5863 : 2006 SOUTH AFRICAN NATIONAL STANDARD Concrete tests — Compressive strength of hardened concrete*. *South African National Standard* (2.1). Pretoria, South Africa: SABS Standards Division. Retrieved from http://store.sabs.co.za/catalogsearch/result/?q=sans+5863

SANS920. (2011). *SANS 920 : 2011 SOUTH AFRICAN NATIONAL STANDARD Steel bars for concrete reinforcing* (2.3). Pretoria, South Africa: SABS Standards Division.

Selander, A. (2010). Hydrophobic Impregnation of Concrete Structures – Effects on Concrete Properties. Retrieved from https://www.diva-portal.org/smash/get/diva2:305538/FULLTEXT02.pdf

Sikagard ® -706 Thixo. (2012). Product Data Sheet. Retrieved from http://www.autospec.co.za/productmedia/sika/thumbnails/datasheets/repair_protection/concrete_protection/sikagard-706-thixo.pdf

Sikalite®. (2012). Product Data Sheet. Retrieved from http://www.autospec.co.za/productmedia/sika/thumbnails/datasheets/repair_protection/concrete_protection/sikagard-706-thixo.pdf

Stern, M., & Geary, A. L. (1957). Electrochemical Polarization. *Journal of The Electrochemical Society*, *104*(9), 559. https://doi.org/10.1149/1.2428653

Tittarelli, F., & Moriconi, G. (2010). The effect of silane-based hydrophobic admixture on corrosion of galvanized reinforcing steel in concrete. *Corrosion Science*, *52*(9), 2958–2963. https://doi.org/10.1016/j.corsci.2010.05.008

Utgenannt, P. (2004). *The Influence of ageing on the salt-frost resistance of concrete*. *Report TVBM 1021; (2004)*. Division of Building Materials, Lund Institute of Technology.

Zhan, H., & Wittmann, F. H. (2005). Relation between the Silicon Resin Profiles in Water Repellent Treated Concrete and the Effectiveness as a Chloride Barrier / Zusammenhang zwischen dem Tiefenprofil des Silikonharzes und der Wirksamkeit einer Hydrophobierung als Chloridschranke. *Restoration of Buildings and Monuments*, *11*(1), 35–46. https://doi.org/10.1515/rbm-2005-5926

Zollo, R. F., & Hays, C. D. (1998). Engineering material properties of a fiber reinforced cellular concrete. *ACI Materials Journal*, *95*(5), 631–635.

# 8 Appendices

## 8.1 Appendix A: Mix Design and Constituents

This appendix includes the main laboratory equipment used in the production of foam and LWFC. In addition to that it also includes the mix design calculation procedure and an excel template that was used throughout the research period to determine the contents of the mixing constituents.

The mix design procedure of LWFC is based on the target density of the material. When specifying LWFC, not only the strength is specified, but also the density. The compressive strength of the material is a function of density, hence the density and strength are closely related. The density can be expressed as either wet or dry density. The mass of the dry mixing constituents and the volume of the foam needed for a certain target density were determined using the equations proposed by Kearsley and Mostert (2005).

These equations equate the relative densities, mass, and volume of the mixing constituents and solve for cement and foam content. For obtaining a cubic metre of LWFC, the total mixing constituents mass must be equal to the required cast density and the total volume of all constituents' material should be one cubic metre. The two equations of density and volume are defined below, as proposed by Kearsley and Mostert (2005).

$$\rho_m = x + x\left(\frac{w}{c}\right) + x\left(\frac{a}{c}\right) + x\left(\frac{s}{c}\right) + x\left(\frac{a}{c}\right)\left(\frac{w}{a}\right) + x\left(\frac{s}{c}\right)\left(\frac{w}{s}\right) + RD_f * V_f \qquad \text{(A.1)}$$

$$1000 = \left(\frac{x}{RD_c}\right) + x\left(\frac{w}{c}\right) + x\left(\frac{\frac{a}{c}}{RD_a}\right) + x\left(\frac{\frac{s}{c}}{RD_s}\right) + x\left(\frac{a}{c}\right)\left(\frac{w}{a}\right) + x\left(\frac{s}{c}\right)\left(\frac{w}{s}\right) + V_f \qquad \text{(A.2)}$$

Where $\rho_m$ = target casting density [kg/m$^3$]

x = cement content [kg/m$^3$]

$\frac{w}{c}$ = water to cement ratio

$\frac{a}{c}$ = ash to cement ratio

$\frac{s}{c}$ = sand to cement ratio

$\frac{w}{s}$ = water to sand ratio

$RD_f$ = relative density of foam

$RD_c$ = relative density of cement

$RD_a$ = relative density of ash

$RD_s$ = relative density of sand

$V_f$ = volume of foam[l]

After all the required mixing constituents were determined, a horizontal 70 litre capacity drum mixer was used for the mixing purposes. And the foam was generated using a foaming machine. Figure A1 and Figure A2 presents the two aforementioned main laboratory equipment used for the preparation of LWFC (i.e. a drum mixer and a foam generator).

Figure A1: LWFC 70 litre drum mixer

Figure A2: Foam generating Machine

### 8.1.1 Materials

#### *8.1.1.1 Binders*

The main binder used to prepare the LWFC was Ordinary Portland Cement (CEM I) 52.5 N, under the brand PPC. The Ordinary Portland Cement (OPC) used complied with the South African National Standard with regards to cement type and strength class (SANS50197-1, 2013). Another binder used was Class S designated fly ash under the brand name ULULA. The Class S fly ash is finer than cement for maximum benefit in the concrete mix and it conformed to the South African Standards (SANS50450-1, 2014). The relative densities of the cement and fly ash were 3.15 kg/m$^3$ and 2.20 kg/m$^3$ respectively.

#### *8.1.1.2 Water*

The water used for both mixing LWFC and preparation of the pre-foam was potable water. This was based on the requirements of the South African Standards (SANS10100-2, 2014), which states that the water should not contain any impurities that may compromise the strength or durability properties of the concrete. Potable water is also recommended when a protein based foaming agent is used to avoid any possible contamination that my affect the quality of the foam (Brady et al., 2001).

#### *8.1.1.3 Foaming Agent and Foam*

A protein based foaming agent with a brand name Foamtech was used to prepare the pre-foam. It was mixed with water at a ratio of 1 litre of foaming agent to 40 litres of water. The foam solution and air were passed through a machine to generate the pre-foam of density 75 kg/m$^3$.

Figure A3: Typical foam produced by the foam generating machine

#### *8.1.1.4 Surface protection systems*

An integral surface treatment was incorporated during the mixing stage of LWFC in one set of the test specimens per mix design. The product used was a silicate-based agent (pore-blocker), brand name Sikalite®. The surface treatment was incorporated by mixing the powdery product mass of 0.2% by weight of the main binder with the dry mix constituents. This was according to the product manufacturer specification as detailed in the product data sheet (Sikalite®, 2012).

Another type of a surface treatment used was a saline-based agent (pore-liner), brand name Sikagard® – 706 Thixo. The surface treatment was applied onto the surface of the specimens after 28 days of curing in a climate-controlled room. The application method was also according to the manufacturer specification (Sikagard ® -706 Thixo, 2012).

#### *8.1.1.5 Fibres*

LWFC is associated with high dry shrinkage strains and low tensile strength. The incorporation of fibres enhances the material's tensile strength and fracture energy (Awang et al., 2012; De Villiers, Van Zijl, & van Rooyen, 2016; Hazlin et al., 2017; Zollo & Hays, 1998). Synthetic polypropylene fibres (SAPY Corehfil™), 12mm in length, were used in the preparation of all the specimens. The fibre content was determined as a percentage volume of 0.45% to all the dry mixing constituents.

Figure A4: Typical 12mm polypropylene fibres used during the production of LWFC

#### *8.1.1.6 Reinforcement*

Rib reinforcing steel bars of diameter Y12 mm were used in the reinforced beam specimens. The symbol 'Y' in front of the diameter value denotes that the reinforcing steel grade was high tensile as prescribed in the South African National Standard(SANS920, 2011). The mass per unit length of the reinforcing bars was 0.888kg. The bars were cut as per shape code 20 (SANS282, 2011) and to an approximate length of 480 mm.

## 8.2 Appendix B: Specimen Cracking Detail

Table 9: Reinforced beam specimen crack detail for mix 1 (ash: cement = 0:1) and reinforcement cover depth of 35mm

| Treatment Type | Beam | Transverse Crack Size & Location | Longitudinal Crack Size |
|---|---|---|---|
| Reference | 1 | **0.2mm** [19.6cm] | **----** |
| | 2 | **0.2mm** [18cm] | ---- |
| | 3 | **0.2mm** [20cm] | ---- |
| surface (Non integral) | 1 | **0.1mm** [15cm]; **0.1mm** [22cm] | ---- |
| | 2 | **0.2mm** [12cm]; **0.1mm** [25cm] | **0.1mm$^{RE}$** |
| | 3 | **0.1mm** [14cm]; **0.2mm** [22cm]; **0.1mm** [30cm] | ---- |
| Integral | 1 | **0.2mm** [19.5cm] | **** |
| | 2 | **0.2mm** [22cm] | ---- |
| | 3 | **0.1mm** [14.5cm]; **0.2mm** [22cm] | ---- |
| | 4 | **0.1mm** [19.5cm] | ---- |

Table 10: Reinforced beam specimen crack detail for mix 1 (ash: cement = 0:1) and reinforcement cover depth of 20mm

| Treatment Type | Beam | Transverse Crack Size & Location | Longitudinal Crack Size |
|---|---|---|---|
| Reference | 1 | **0.15-0.2mm** [21.6cm] | **0.4mm** |
| | 2 | **0.15mm** [25cm] | **0.1mm$^{RE}$** |
| | 3 | **0.1mm** [6cm]; 0**.2mm** [16.4cm]; **0.2mm** [27cm] | ---- |
| surface (Non integral) | 1 | **0.2mm** [20cm] | **0.1mm$^{RE}$** |
| | 2 | **0.1mm** [7.5cm]; **0.1mm** [16.5cm]; **0.2mm** [25cm] | **0.2mm$^{RE}$** |
| | 3 | **0.1mm** [9.5cm]; **0.2mm** [20.5cm]; **0.1mm** [32cm] | **0.1mm$^{LE}$** |
| Integral | 1 | **0.2mm** [23cm] | **0.1mm$^{RE}$** |
| | 2 | **0.15mm** [23cm] | **0.2mm$^{LE}$** ; **0.1mm$^{RE}$** |
| | 3 | **0.2mm** [15.6cm] | **0.2mm$^{LE}$** ; **0.1mm$^{RE}$** |

Table 11: Reinforced beam specimen crack detail for mix 2 (ash: cement = 1:1) and reinforcement cover depth of 35mm

| Treatment Type | Beam | Transverse Crack Size & Location | Longitudinal Crack Size |
|---|---|---|---|
| Reference | 1 | ---- | ---- |
| | 2 | **0.2mm** [18cm] | ---- |
| | 3 | **0.1mm** [28cm] | ---- |
| | 4 | ---- | |
| surface (Non integral) | 1 | **0.1mm** [15cm]; **0.1mm** [22cm] | ---- |
| | 2 | **0.2mm** [12cm]; **0.1mm** [25cm] | **0.1mm**$^{LE}$ |
| | 3 | **0.1mm** [14cm]; **0.2mm** [22cm]; **0.1mm** [30cm] | ---- |
| Integral | 1 | **0.2mm** [19.5cm] | **0.1mm**$^{LE\ \&\ RE}$ |
| | 2 | **0.1mm** [35cm] | **0.1mm**$^{LE}$ |
| | 3 | ---- | **0.1mm**$^{LE\ \&\ RE}$ |

Table 12: Reinforced beam specimen crack detail for mix 2 (ash: cement = 1:1) and reinforcement cover depth of 20mm

| Treatment Type | Beam | Transverse Crack Size & Location | Longitudinal Crack Size |
|---|---|---|---|
| Reference | 1 | **0.1mm** [24cm] & [36cm] | ---- |
| | 2 | **0.1mm** [12.5cm]; **0.15mm** [32.5cm] | **0.1mm**$^{RE}$ |
| | 3 | **0.1mm** [18cm] | **0.1mm**$^{**}$ |
| | 4 | **0.1mm** [23.5cm] | |
| surface (Non integral) | 1 | **0.2mm** [20cm] | **0.1mm**$^{RE}$ |
| | 2 | **0.1mm** [7.5cm]; **0.1mm** [16.5cm]; **0.1mm** [25cm] | **0.2mm**$^{RE}$ |
| | 3 | **0.1mm** [9.5cm]; **0.2mm** [20.5cm]; **0.1mm** [32cm] | **0.1mm**$^{LE}$ |
| Integral | 1 | **0.1mm** [18.5cm] | **0.1mm**$^{RE}$ |
| | 2 | **0.1mm** [30cm] | **0.1mm**$^{LE\ \&\ RE}$ |
| | 3 | **0.2mm** [18.6cm] | **0.1mm**$^{RE*}$ |

Table 13: Reinforced beam specimen crack detail for mix 3 (ash: cement = 2:1) and reinforcement cover depth of 35mm

| Treatment Type | Beam | Transverse Crack Size & Location | Longitudinal Crack Size |
|---|---|---|---|
| Reference | Beam 10 | **0.1mm** [26cm] | **----** |
| | Beam 11 | ---- | ---- |
| | Beam 12 | ---- | ---- |
| surface (Non integral) | 5 | **0.1mm** [14cm]; **0.1mm** [22cm] | **0.1mm** |
| | Beam 11 | **0.1mm** [11cm] | ---- |
| | Beam 12 | ---- | ---- |
| Integral | Beam 9 | ---- | **0.1mm** |
| | Beam 10 | **0.1mm** [22cm] | ---- |
| | Beam 12 | **0.1mm** [14.5cm]; **0.1mm** [22cm] | ---- |
| | Beam 11 | **0.1mm** [19.5cm] | ---- |

Table 14: Reinforced beam specimen crack detail for mix 3 (ash: cement = 2:1) and reinforcement cover depth of 20mm

| Treatment Type | Beam | Transverse Crack Size & Location | Longitudinal Crack Size |
|---|---|---|---|
| Reference | Beam 1 | **0.1mm** [18cm] | ---- |
| | Beam 2 | ---- | ---- |
| | Beam 3 | ---- | ---- |
| surface (Non integral) | Beam 1 | ---- | **0.1mm** |
| | Beam 2 | ---- | ---- |
| | Beam 3 | ---- | ---- |
| Integral | Beam 1 | **0.1mm** [16cm] | ---- |
| | Beam 2 | **0.1mm** [20cm]; **0.1mm** [32cm] | ---- |
| | Beam 3 | **0.1mm** [15.6cm] | **0.1mm** |

## 8.3 Appendix C: Concentration Calculations

Presented below are the chemical calculations for the concentration of silver nitrate and sodium chloride solutions used in the course of this study.

Concentration calculations

$AgNO_3$ ⟹

$M_r(AgNO_3) = 169.8731$ g/mol

$$C = \frac{m}{V} \times \frac{1}{M_r}$$

m → mass
V → volume
$M_r$ → molar mass
C → concentration

$$0.1 = \frac{m(g)}{1L} \times \frac{1}{169.8731}$$

$m = 16.98731$ g

Dilute 16.98 g of $AgNO_3$ into 1L of water to get 0.1M $AgNO_3$ solution

NaCl ⟹

$M_r(NaCl) = 58.44$ g/mol

$$C = \frac{M}{V} \times \frac{1}{M_r}$$

$$0.3 = \frac{m}{1L} \times \frac{1}{58.44}$$

$m = 17.532$ g

Dilute 17.532 g of NaCl into 1L of water to get 0.3M NaCl solution.

## 8.4 Appendix D: Fly Ash Data Sheet

2008/005640/07
ULULA ASH (Pty)Ltd
P O Box 1516
Silverton 0127
Tel : 011 708 0010
Fax : 086 545-4671

**ULULA ASH**
**KRIEL POWER STATION**

**TEST CERTIFICATE for Class S Fly Ash (SFA)**

**The values shown below are from results obtained between Feb 2015 to Oct 2015 from our** ongoing quality management systems as required by the South African National Standard {SANS}
**SANS 50450-1:2011 Fly Ash for Concrete (Siliceous Fly Ash)**

| Chemical Requirements | Tested percentages | Specification SANS 50450-1:2011 |
|---|---|---|
| Loss of ignition | 0,8 - 1,6 | Max. 5,0% by mass |
| Chloride content ($Cl^-$) | <0.05 | Max. 0,10% by mass |
| Sulfuric anhydride ($SO_3$) | 0,8 - 1,2 | Max. 3,0% by mass |
| Free calcium oxide ** | 1,4 - 2,3% | Max. 2,5% ** or 1,0% by mass |
| Calcium oxide | 6,0 - 9,5 | Max. 10,0% by mass |
| Reactive calcium oxide | Not required | Calcium oxide < 10% |
| Chloride content ($Cl^-$) | <0.1 | Max. 0,10% by mass |
| Reactive silicon dioxide | Not required | No co-combustion |
| Si. dioxide, Al. oxide and Ir. oxide | Not required | No co-combustion |
| $Na_2O$ (equivalent) | Not required | No co-combustion |
| Magnesium oxide (MgO) | Not required | No co-combustion |
| Soluble phosphate ($P_2O_5$) | Not required | No co-combustion |

| Physical Requirements | Test results | Specification SANS 50450-1:2011 |
|---|---|---|
| Fineness retained on the 45 micron sieve | 10,0 - 11,5 % | Max. 12,0% by mass |
| Activity index | 80 - 86 % | Min. 75% @ 28 days |
| Activity index | 95 - 103 % | Min. 85% @ 90 days |
| Soundness, expansion ** | < 0,1 mm | Max. of 10 mm |
| Particle density | 2250kg/m3 | Max. +-200kg/m³ of declaration |
| Initial setting times | Not required | No co-combustion |
| Water requirement | 92 - 94 % | Max. 95% by mass of control |

Directors: C.D Billett, M.F.Hovy, A. Thedvall

**Additional information;**

| Chemical Composition | Typical percentages |
|---|---|
| $SiO_2$ | 50,0 - 52,5 |
| $Al_2O_3$ | 28,5 - 30,5 |
| $Fe_2O_3$ | 2,0 - 3,0 |
| CaO | 6,0 - 9,5 |
| MgO | 2,0 - 2,5 |
| $K_2O$ | < 1 |
| Na Equivalent | < 1.5 |
| $TiO_2$ | 1,5 - 2,0 |

Date issued: 3 February 2016
Issued by: Mark Hovy

**Your attention is drawn to the fact that PPC Group Laboratory Services has been contracted by us to do our product conformance testing according to the relevant SANS test methods.**

**a SANAS testing laboratory no. T0241.**

Directors: C.D Billett, M.F.Hovy, A. Thedvall

## 8.5 Appendix E: Surface Treatment Agents Date Sheet

### 8.5.1 Sikagard-706 Thixo (pore-liner)

**Product Data Sheet**
Edition 21/02/2012
Identification no:
02 03 03 01 002 0 000003
Sikagard®-706 Thixo

Construction

# Sikagard®-706 Thixo

## Silane based water repellent impregnation cream

| | |
|---|---|
| **Product Description** | Sikagard®-706 Thixo is a one part reactive silane based impregnation cream. It is a solvent free product with ~ 80% content of active substance. Sikagard®-706 Thixo complies with the highest requirements of EN 1504-2 for hydrophobic Impregnation (penetration depth class II & resistance to freeze and thaw salt stresses). |
| **Uses** | Sikagard®-706 Thixo is used as water-repellent impregnation (hydrophobic treatment) for absorbent substrates such as concrete in civil engineering or building concrete structures subjected to heavy stress due to freeze and thaw cycles and de-icing salts, chloride attack in marine environment, etc…<br>√ Suitable for protection against ingress (Principle 1, method 1.1 of EN 1504-9)<br>√ Suitable for moisture control (Principle 2, method 2.1 of EN 1504-9)<br>√ Suitable for increasing the resistivity (Principle 8, method 8.1 of EN 1504-9) |
| **Characteristics / Advantages** | ■ Non-sag (thixotropic) consistency, allowing wastage-free application of sufficient quantities and assuring deep penetration<br>■ Reduction of water absorption<br>■ Reduction of absorption of aggressive or deleterious agents dissolved in water (i.e. de-icing salts or chloride from marine environment)<br>■ No noticeable change of water vapour permeability<br>■ Not film forming<br>■ Ready for use<br>■ Long term efficiency, deep penetration<br>■ Increases the resistance of concrete to freeze and thaw cycles and de-icing salts<br>■ Resistant to sea water<br>■ Low VOC content |
| **Tests** | |
| **Approvals / Standards** | Conforms to the requirements of LPM-qualification test to SIA 162/5, Report A-20 450-1 of 19.04.1999. (Water absorption, penetration depth, alkali resistance, water vapour diffusion, resistance to freeze thaw cycles and de-icing salts).<br>Conforms to the requirement of the "Bro 2002" Swedish National Road Administration (SNRA) publication No. VV2002:47 –report reference F507580 Arev<br>Conforms to the requirements of the EN 1504-2 class II – Polymer Institute report P 5672-E dated 9th August 2007. |

## Product Data

### Form

| | |
|---|---|
| **Appearance / Colour** | White paste / cream (transparent after application and drying) |
| **Packaging** | 18 kg and 180 kg containers |

### Storage

| | |
|---|---|
| **Storage Conditions / Shelf Life** | 12 months from date of production if stored in undamaged and unopened original sealed packaging in dry and cool conditions. |

### Technical Data

| | | |
|---|---|---|
| **Chemical Base** | Silane (~ 80% active ingredient) | |
| **Density** | ~ 0.900 kg/l (at +20°C) | |
| **pH Value** | ~ 8 | |
| **VOC** | ~ 77 g/lt (~ 0.77% w/w) | |
| **Resistance to Freeze-Thaw-Salts Stress** | Comply | (EN 13581) |
| **Depth of Penetration** | Class II: ≥ 10 mm Test performed on concrete with a W/C = 0.70 | |
| **Water Absorption** | <7.5% | (EN 13580) |
| **Drying Rate Coefficient** | Class I: > 30% | (EN 13579) |

### Resistance

| | | |
|---|---|---|
| **Alkali Resistance** | < 10% | (EN 13580) |

## System Information

| | |
|---|---|
| **System Structure** | 1 - 2 coats of Sikagard®-706 Thixo |

### Application Details

| | |
|---|---|
| **Consumption** | Dependent on substrate profile and porosity as well as the required penetration depth: ~ 200 to 300 g/m$^2$ per coat. |
| **Substrate Quality** | Free of dust, dirt, oil, efflorescence and existing paint coats.<br>Cracks in concrete more than 200 microns must be repaired prior to application of the hydrophobic treatment. |
| **Substrate Preparation** | Cleaning is best done with suitable detergents or by light blastcleaning, steam cleaning etc.<br>Best results are obtained on dry, very absorbent substrates. The substrate must look dry with no damp patches. |

### Application Conditions / Limitations

| | |
|---|---|
| **Substrate Temperature** | +5°C min. / +35°C max. |
| **Ambient Temperature** | +5°C min. / +40°C max. |

### Application Instructions

| | |
|---|---|
| **Mixing** | Sikagard®-706 Thixo is supplied ready for use and should not be thinned or diluted. |

Construction

| | |
|---|---|
| **Application Method / Tools** | Sikagard®-706 Thixo is applied using airless spray, brush or roller, from top to bottom in a single pass. |
| **Cleaning of Tools** | Clean all tools and application equipment with Colma Cleaner immediately after use. Hardened / cured material can only be mechanically removed. |
| **Waiting Time / Overcoating** | Can be overcoated with water and solvent based polymer paint - contact the proposed paint manufacturer for recommendations.<br>Sikagard®-706 Thixo can be used as water repellent primer under many Sikagard® protective coatings. Penetration of water is thus prevented at possible weak spots or in the event of damage to the top coat and the risk of consequential damages such as paint flaking can be reduced.<br>Waiting time: minimum 5 hours, maximum 1 week. |
| **Notes on Application / Limitations** | Best results are achieved when Sikagard®-706 Thixo is applied on 28 days old concrete – however, due to its high alkali resistance, it is still possible to apply it at a very early age.<br>Areas such as window frames which still need to be painted must be securely covered to avoid contact with Sikagard®-706 Thixo.<br>Areas not to be impregnated such as window panes need to be protected from being accidentally contaminated with Sikagard®-706 Thixo.<br>Sikagard®-706 Thixo can damage some coatings and bituminous products.<br>Sikagard®-706 Thixo can lead to darkening of concrete, apply sample areas first.<br>Cannot be overcoated with limewash or cement paint.<br>Apply Sikagard®-706 Thixo onto a sample area to confirm consumption rates.<br>Refer to the latest Method Statement for detailed information regarding surface preparation, application method, etc. |

## Curing Details

| | |
|---|---|
| **Curing Treatment** | Sikagard®-706 Thixo does not require any special curing but must be protected from rain for at least 3 hours at +20°C. |

## Value Base

All technical data stated in this Product Data Sheet are based on laboratory tests. Actual measured data may vary due to circumstances beyond our control.

## Local Restrictions

Please note that as a result of specific local regulations the performance of this product may vary from country to country. Please consult the local Product Data Sheet for the exact description of the application fields.

## Health and Safety Information

For information and advice on the safe handling, storage and disposal of chemical products, users should refer to the most recent Material Safety Data Sheet containing physical, ecological, toxicological and other safety-related data.

## Legal Notes

The information, and, in particular, the recommendations relating to the application and end-use of Sika products, are given in good faith based on Sika's current knowledge and experience of the products when properly stored, handled and applied under normal conditions in accordance with Sika's recommendations. In practice, the differences in materials, substrates and actual site conditions are such that no warranty in respect of merchantability or of fitness for a particular purpose, nor any liability arising out of any legal relationship whatsoever, can be inferred either from this information, or from any written recommendations, or from any other advice offered. The user of the product must test the product's suitability for the intended application and purpose. Sika reserves the right to change the properties of its products. The proprietary rights of third parties must be observed. All orders are accepted subject to our current terms of sale and delivery. Users must always refer to the most recent issue of the local Product Data Sheet for the product concerned, copies of which will be supplied on request or access on the Internet under www.sika.co.za.

Sika South Africa (Pty) Ltd
9 Hocking Place,
Westmead, 3608
South Africa

E-mail: headoffice@za.sika.com
Phone +27 31 792 6500
Telefax +27 31 700 1760
www.sika.co.za

## 8.5.2 Sikalite (pore-blocker)

Construction

**Product Data Sheet**
Edition 21/02/2012
Identification no:
010705040010000002
Sikalite®

# Sikalite®

## Powdered waterproofing admixture for mortar

| | |
|---|---|
| **Product Description** | Sikalite® is a powdered waterproofing admixture, which blocks the capillaries and pores in Portland cement/sand mortars preventing the movement of moisture. |
| **Uses** | Sikalite® is used to waterproof Portland cement/sand renders and mortars for application to:<br>■ Walls<br>■ Facades<br>■ Floor toppings<br>■ Jointing mortars |
| **Characteristics / Advantages** | ■ Easy to use<br>■ Economical<br>■ Convenient powdered form<br>■ Watertight, but vapour permeable<br>■ Chloride free |

### Product Data

| | | |
|---|---|---|
| **Form** | | |
| **Appearance / Colour** | Powder | Beige |
| **Packaging** | 1, 25 and 200kg units | |
| **Storage** | | |
| **Storage Conditions / Shelf-Life** | 12 Months in original, unopened container. Store in a dry area between 5ºC and 40ºC. Protect from direct sunlight. | |

### Technical Data

| | |
|---|---|
| **Density** | 0,9kg/litre |
| **Application Details** | |
| **Consumption / Dosage** | 1kg per 50 kg of Portland cement i.e. 2% by weight of cement. |

## Application Instruction

**Mixing (Ratio/Dosage)**

**SUGGESTED MIX PROPORTIONS**

Building Mortar

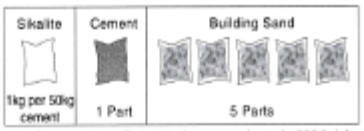


1 Pocket of cement is sufficient to lay approximately 300 bricks

External Plaster

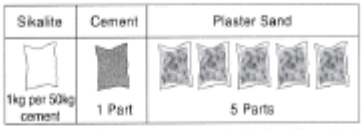


1 pocket of cement will cover approximately 10m² at 15mm thick

Floor Screed

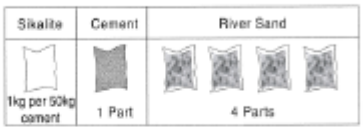


1 pocket of cement will cover approximately 4m² at 25mm thick

**Notes on Application / Limits**

Sikalite® is added to the dry mix of Portland cement and sand prior to the addition of the gauging water. Overdosing can cause retardation of set.

The quality and waterproofness of the cement mortar mixes may be affected by one or more of the following:

- Poor quality sand
- Poorly graded sand
- Excessive dust in the sand
- Excess water
- Excess cement
- Lack of adequate curing

We recommend you consult with your nearest Cement and Concrete Institute office who will provide you with the correct information regarding sand types and gradings.

**Curing Details**

**Curing Treatment**

Apply correct curing procedures.

**Local Restrictions**

Please note that as a result of specific local regulations the performances of this product may vary from country to country. Please consult the local Product Data Sheet for the exact description of the application fields.

## Health and Safety Information

**Protective Measures**

Contact with skin and eyes must be avoided.

**Ecology**

**Transportation Class**

**Important Notes**

Residues of material must be removed according to local regulations. Fully cured material can be disposed of as household waste under agreement with the responsible local authorities.

Detailed health and safety information as well as detailed precautionary measures e.g. physical, toxicological and ecological data can be obtained from the Material Safety Data Sheet.

**Toxicity**

Construction

| | |
|---|---|
| **Legal Notes** | The information, and, in particular, the recommendations relating to the application and end-use of Sika® products, are given in good faith based on Sika's current knowledge and experience of the products when properly stored, handled and applied under normal conditions. In practice, the differences in materials, substrates and actual site conditions are such that no warranty in respect of merchantability or of fitness for a particular purpose, nor any liability arising out of any legal relationship whatsoever, can be inferred either from this information, or from any written recommendations, or from any other advice offered. The proprietary rights of third parties must be observed. All orders are accepted subject to our current terms of sale and delivery. Users must always refer to the most recent issue of the Product Data Sheet for the product concerned, copies of which will be supplied on request or accessed on the Internet under www.sika.co.za. |

Sika South Africa (Pty) Ltd
9 Hocking Place,
Westmead, 3608
South Africa

E-mail: headoffice@za.sika.com
Phone +27 31 792 6500
Telefax +27 31 700 1760
www.sika.co.za